ENVI-MET
principi fisici della modellazione del comfort outdoor

Kristian Fabbri - 29 Settembre 2017

Homepage del software

Headquarter

Accesso veloce alla homepage del software e cabina di pilotaggio della modellazione

Leonardo 2014

Analizza I tuoi risultati e crea una mappa 2D e 3D

Spaces

Disegna il tuo progetto e l'ambiente

BioMet

Sistema di processo per i file di out put per calcolare PMV/PPD, PET o UTCI

Comfort: Modellazione e progetto architettonico-urbanistico

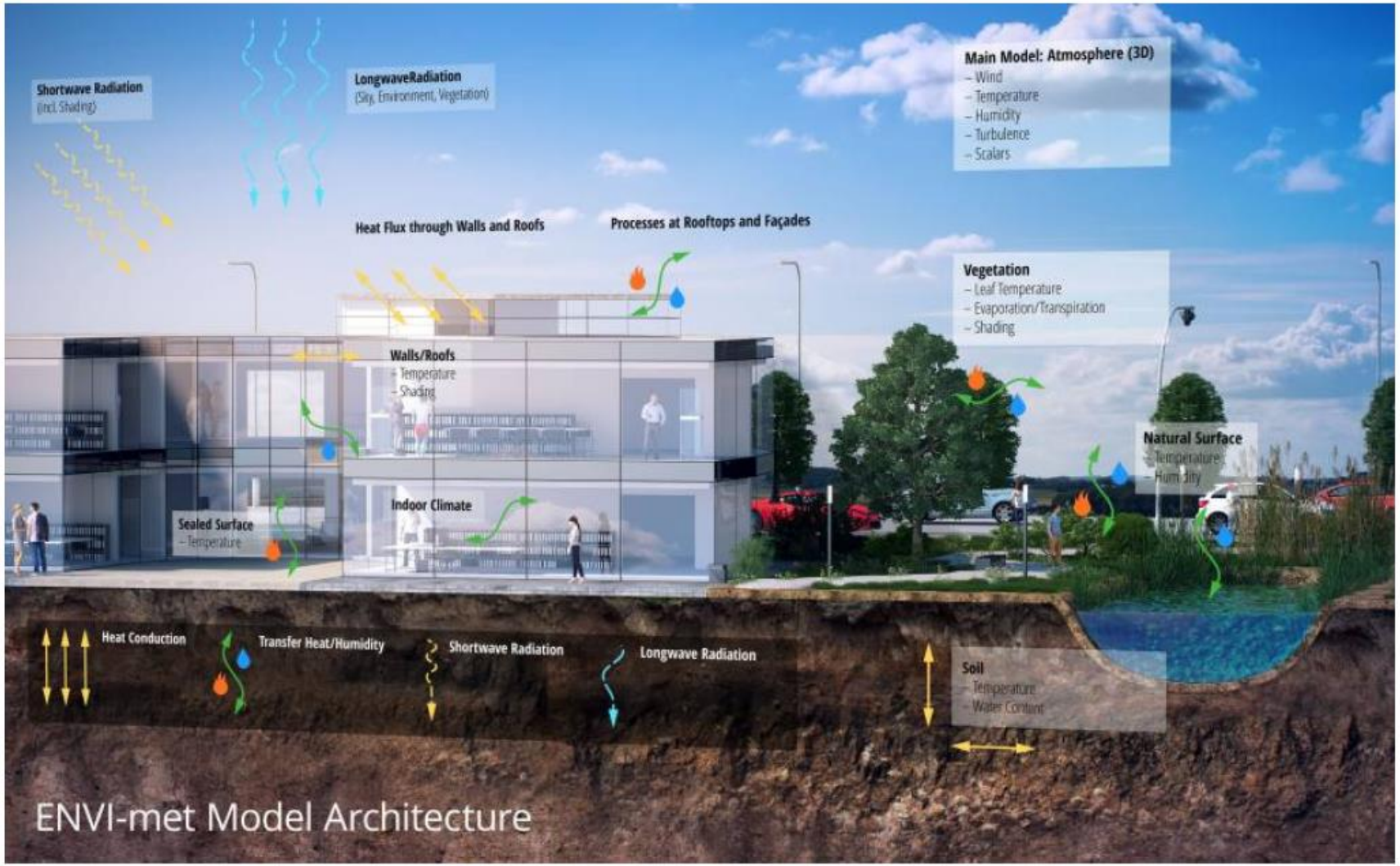

Struttura del software

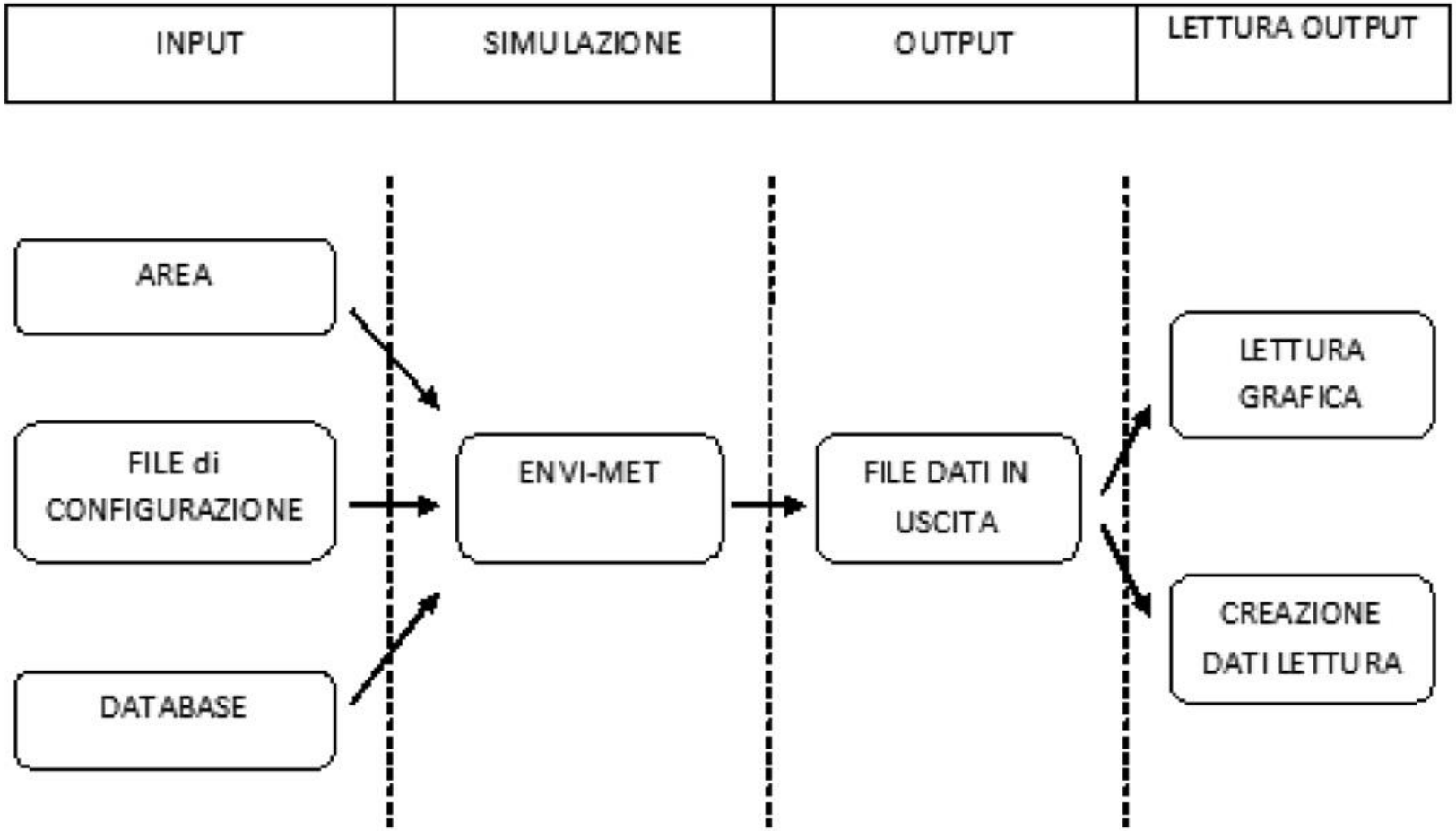

Equazioni

Boundary conditions: A *no-slip* condition is used for all solid surfaces. The inflow profile is obtained from the one-dimensional reference model and a zero-gradient Neumann condition is used at the outflow and lateral boundaries. At the top boundary all vertical motions are assumed to be zero. Special boundary conditions are used for the pressure perturbation on all outflow boundaries to keep the model mass conserving.

$$\frac{\partial u}{\partial t} + u_i \frac{\partial u}{\partial x_i} = -\frac{\partial p}{\partial x} + K_m \left(\frac{\partial^2 u}{\partial {x_i}^2} \right) + f\left(v - v_g\right) - S_u$$

$$\frac{\partial v}{\partial t} + u_i \frac{\partial v}{\partial x_i} = -\frac{\partial p}{\partial y} + K_m \left(\frac{\partial^2 v}{\partial {x_i}^2} \right) - f\left(u - u_g\right) - S_v$$

$$\frac{\partial w}{\partial t} + u_i \frac{\partial w}{\partial x_i} = -\frac{\partial p}{\partial z} + K_m \left(\frac{\partial^2 w}{\partial {x_i}^2} \right) + g \frac{\theta(z)}{\theta_{ref}(z)} - S_w$$

Temperature and Humidity

The distribution of the air temperature and specific humidity q is given by the combined advection diffusion equation with internal source/sinks

$$\frac{\partial u}{\partial x} + \frac{\partial v}{\partial y} + \frac{\partial w}{\partial z} = 0$$

Atmospheric turbulence

Turbulence is produced when the air flow is sheared at building walls or vegetation elements. Under windy conditions, the magnitude of local turbulence production normally surpasses its dissipation, so that turbulent eddies are transported by the mean air flow. Depending on the structure of the flow, this leads to an increased turbulence away from the original source of disturbance. *To simulate this effect, a so-called 1.5 order turbulence closure model is used in ENVI-met. Based on the work of Mellor and Yamada (1975) two additional prognostic variables, the local turbulence (E) and its dissipation rate (∑) are added to the model.*

$$\frac{\partial \theta}{\partial t} + u_i \frac{\partial \theta}{\partial x_i} = K_h \left(\frac{\partial^2 \theta}{\partial {x_i}^2} \right) + \frac{1}{c_p \rho} \frac{\partial R_{n,lw}}{\partial z} + Q_h$$

$$\frac{\partial q}{\partial t} + u_i \frac{\partial q}{\partial x_i} = K_q \left(\frac{\partial^2 q}{\partial {x_i}^2} \right) + Q_q$$

La modellazione della vegetazione

La vegetazione viene trattata come una colonna mono dimensionale con altezza Zp nella La vegetazione è trattata come una colonna monodimensionale di altezza zp in cui il profilo della densit{ d'area delle foglie (LAD) è usato per descrivere la densità e la distribuzione delle foglie.
Lo stesso concetto è usato, all'interno del suolo, fino ad una profondità –zr, per descrivere la distribuzione delle radici, attraverso il RAD (Root Area Density).
Questo schema universale può essere applicato sia alle piante ad alto fusto, sia ai cespugli, sia all'erba, semplicemente associando ad ogni tipo di pianta i proprio valori di zp e zr.

Dominio computazionale e la struttura della griglia

A seconda del problema, la dimensione totale del modello tridimensionale X, Y e Z, nonché la risoluzione della griglia può essere selezionata entro un ampio intervallo. Per impostazione predefinita, la spaziatura □x, □y e □z è equidistante in ogni direzione (solo la cella più bassa al di sopra del suolo è normalmente suddivisa in 5 sotto-cellule con il formato $\Delta z_g = 0.2\Delta z$ per aumentare la precisione nel processo di calcolo della superficie).
Il modello tridimensionale è annidato in un modello unidimensionale che si estende fino a 2500 m altezza. I valori di un modello tridimensionale sono utilizzati come valori di riferimento come anche i profili di afflusso e le condizioni al contorno per il modello tridimensionale.

Rotazione del modello

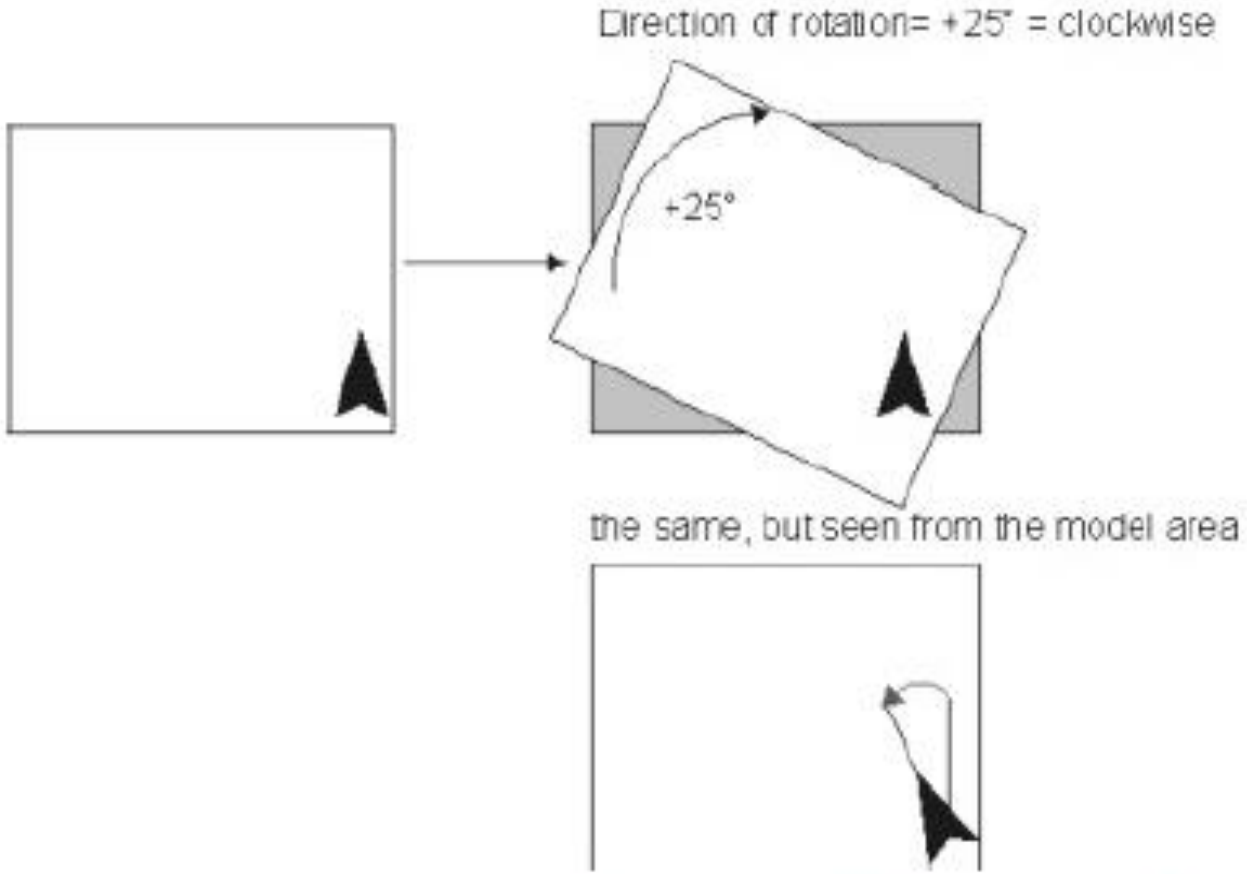

Griglia verticale

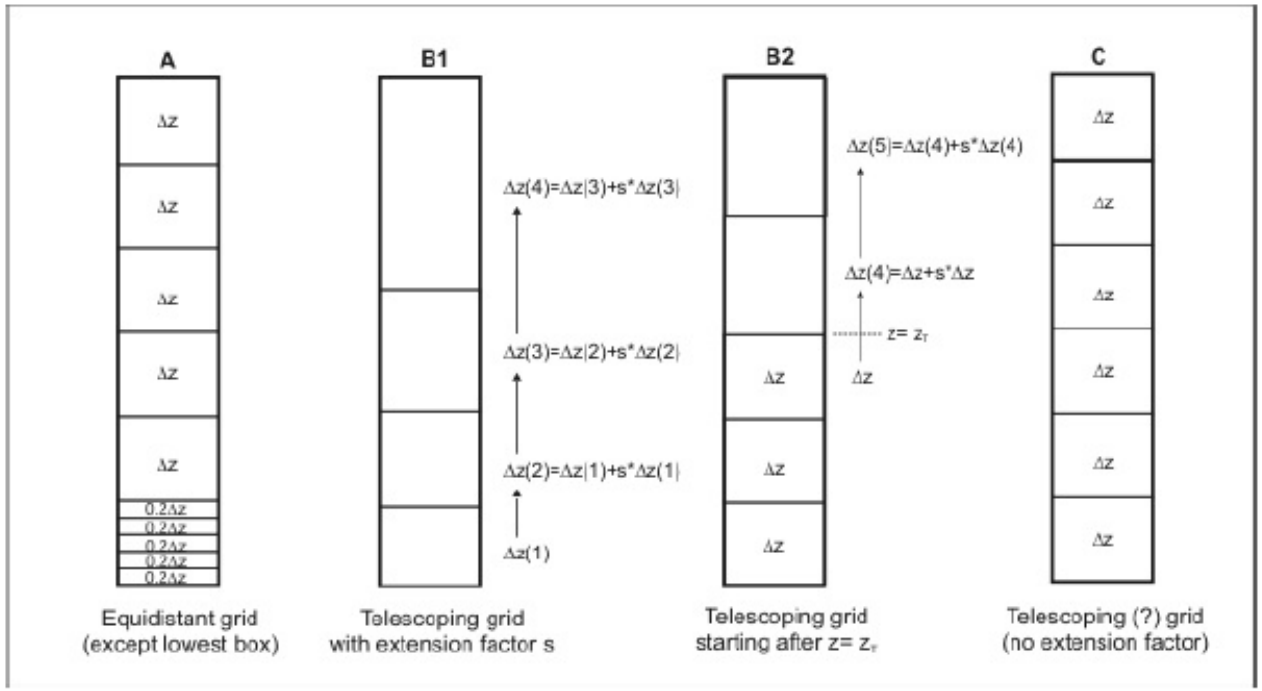

Different concepts for organizing the vertical grid layout: (A): Equidistant Grid, (B): Telescoping grid and (C): Telescoping grid with no extension factor

Nei modelli 3D completi la griglia verticale è fissata una volta creato il modello. L'unico modo per cambiarla è di convertire il modello verso il basso per un modello 2.5D (e perdere tutte le informazioni del 3D), modificare le impostazioni di rete e poi ri-convertirlo in 3D. In breve, quando si crea un modello 3D si dovrebbe pensare alla messa a punto della griglia verticale in dettaglio PRIMA di iniziare a modificare il modello.

La modellazione dela turbolenza

Si basa su due variabili: la turbolenza locale (E) e il suo tasso di dissipazione (ε).
L'energia cinetica in questo caso rappresenta una misura dell'intensità delle turbolenze dell'aria; essa risulta direttamente legata al trasporto locale di calore e umidità.

Il sistema implementato è di due equazioni di cui la prima descrive la distribuzione di energia cinetica nell'aria in funzione della produzione dei moti convettivi e la seconda esprime la dissipazione dell'energia stessa.

$$\frac{\partial E}{\partial t} + u\frac{\partial E}{\partial x} + v\frac{\partial E}{\partial y} + w\frac{\partial E}{\partial z} =$$
$$\frac{\partial}{\partial x}\left(K_E\frac{\partial E}{\partial x}\right) + \frac{\partial}{\partial y}\left(K_E\frac{\partial E}{\partial y}\right) + \frac{\partial}{\partial z}\left(K_E\frac{\partial E}{\partial z}\right)$$
$$+ K_m\left\{2\left(\frac{\partial u}{\partial x}\right)^2 + \left(\frac{\partial u}{\partial y} + \frac{\partial v}{\partial x}\right)^2 + \left(\frac{\partial u}{\partial z} + \frac{\partial w}{\partial x}\right)^2 + 2\left(\frac{\partial v}{\partial y}\right)^2\right.$$
$$\left. + \left(\frac{\partial v}{\partial z} + \frac{\partial w}{\partial y}\right)^2 + 2\left(\frac{\partial w}{\partial z}\right)^2\right\} - \frac{g}{\bar{\theta}}K_h\frac{\partial \theta}{\partial z} + Q_E(x,y,z) - \epsilon$$

on is similar but describes the Dissipation Rate of TKE (ε or eps):

$$\frac{\partial \epsilon}{\partial t} + u\frac{\partial \epsilon}{\partial x} + v\frac{\partial \epsilon}{\partial y} + w\frac{\partial \epsilon}{\partial z} = \frac{\partial}{\partial x}\left(K_\epsilon\frac{\partial \epsilon}{\partial x}\right) + \frac{\partial}{\partial y}\left(K_\epsilon\frac{\partial \epsilon}{\partial y}\right) + \frac{\partial}{\partial z}\left(K_\epsilon\frac{\partial \epsilon}{\partial z}\right)$$
$$+ c_{1\epsilon}\frac{\epsilon}{E}K_m\left\{2\left(\frac{\partial u}{\partial x}\right)^2 + \left(\frac{\partial u}{\partial y} + \frac{\partial v}{\partial x}\right)^2 + \left(\frac{\partial u}{\partial z} + \frac{\partial w}{\partial x}\right)^2 + 2\left(\frac{\partial v}{\partial y}\right)^2\right.$$
$$\left. + 2\left(\frac{\partial v}{\partial y}\right)^2 + \left(\frac{\partial v}{\partial z} + \frac{\partial w}{\partial y}\right)^2 + 2\left(\frac{\partial w}{\partial z}\right)^2\right\}$$
$$- c_{3\epsilon}\frac{\epsilon}{E}\cdot\frac{g}{\bar{\theta}}K_h\frac{\partial \theta}{\partial z} - c_{2\epsilon}\frac{\epsilon^2}{E} + Q_\epsilon(x,y,z)$$

La nesting grid

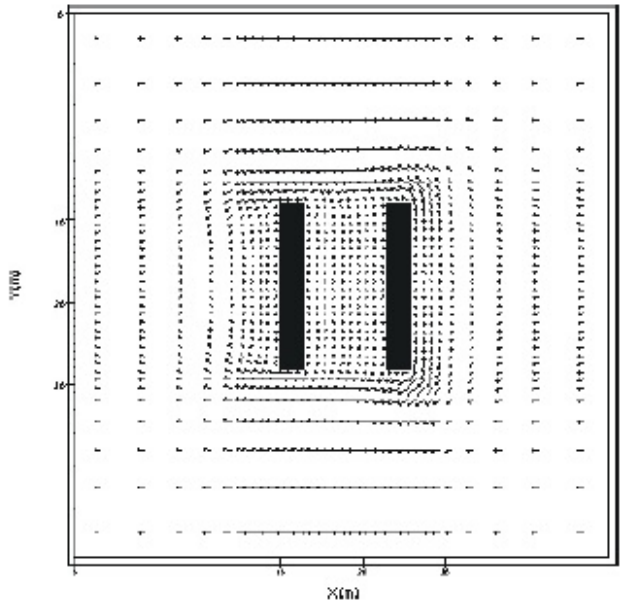

Figure B: (Better) Flow around two Buildings with 5 Nesting Grids

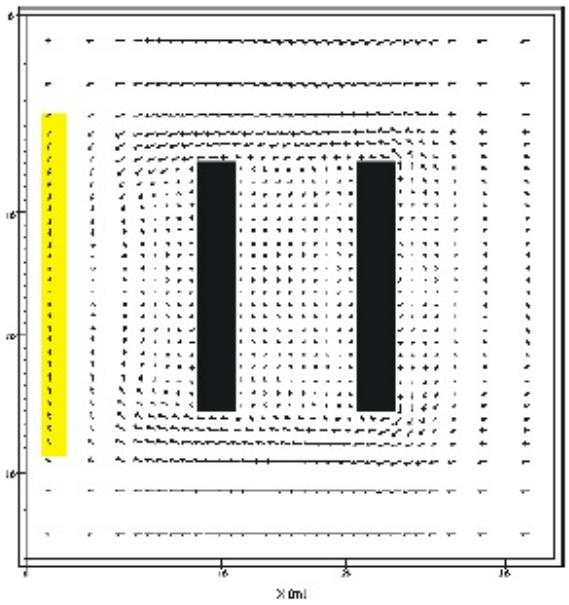

Figure A - Flow around two Buildings with 3 Nesting Grids

The Role of Nesting Grids

The only difference between example A and B is that in (A) we have used only 3 nesting grid cells around the core domain whereas in (B) 5 of them are used. As the grid size of the nesting grids is increasing with each grid, the area is extending very fast with each extra Nesting Grid. The Remember: The Gesting Grids are not included in the Output Files by default, so you will not be able to see troubles there. To see the complete model area, you must include the nesting grids in the Output Files

Layout di Envi - met

Basic Layout of ENVI-met

The sketch above aims to give you an impression over the very basic structure of a microclimate model like ENVI-met.

The general design is not only specific to ENVI-met but is used by almost all 3D numerical models.

The Main Model is designed in 3D with 2 horizontal dimensions (x and y) and one vertical dimension (z). Inside this main model, the typical elements that represent the area of interest are placed: buildings, vegetation, different types of surfaces. To use a numerical model, the area of interest must be reduced into grid cells. The smaller one single grid cell is, the finer the resolution of the model is. On the other hand, making the grid cells small means that more cells are needed to cover a certain area.

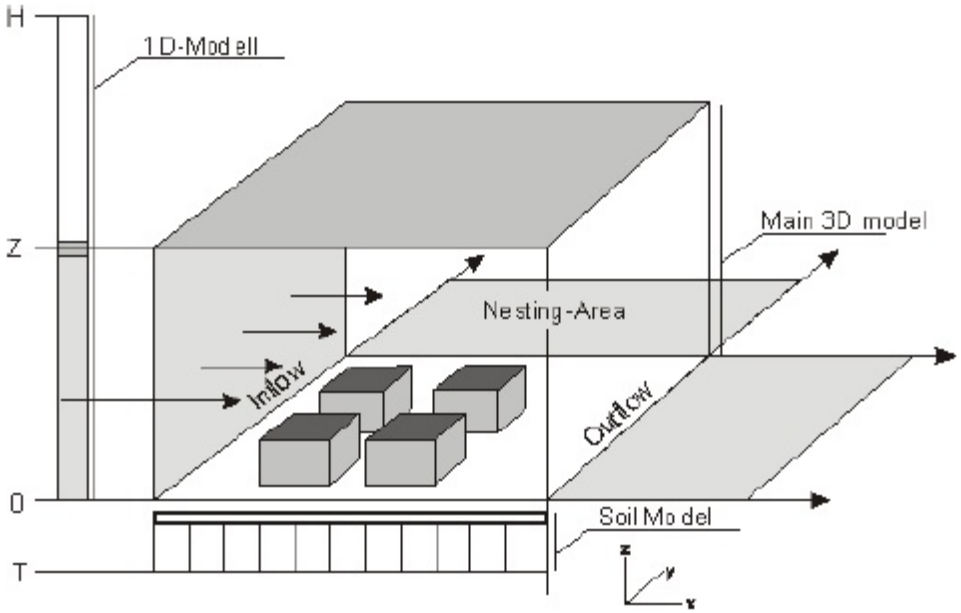

For example, a 100 x 100 m area can be organised in 100 x 100 grid cells of 1 x 1 m each or it can be organised in 20 x 20 grid cells with 5 x 5 m each. For each simulation, a compromise has to be found between the accuracy and resolution of the model and the number of treatable grid cells. As a rule of thumb, reaching 250 x 250 x 30 grid cells (or any other combination such as 120 x 80 x 30,…) ***can be considered as a large model needing a good amount of CPU time.***

Total Model Height

What is the Minimum Model Height?

Selecting the correct size of the model domain is a central aspect in successful numerical modelling.

Whereas the horizontal dimension is more or less given by the dimension of your subject of interest, the vertical height of the model is less obvious and can - if not selected properly - cause
major problems.

The height of the 3D model is a result of the number of vertical grid points used as defined in the Area Input File and grid size plus the method of grid creation (see also Model Layout).

A simple Example: If you have a 30 m building in your model and you choose to have 10 grids with a grid size of 2 m each, the total model height will be 20 m, or, in other words, your building will look 10 m out of the model domain. This is, of course, not acceptable.

Boundary layer

Lateral boundary conditions (LBC) define the way, the model behaves at its lateral boundaries. This is a very specific setting and you normally do not need to change these settings.

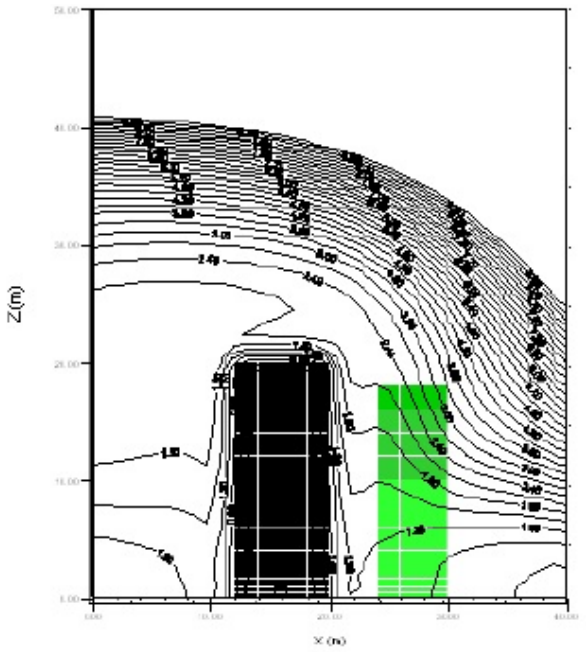

Km distribution for forced/closed LBC

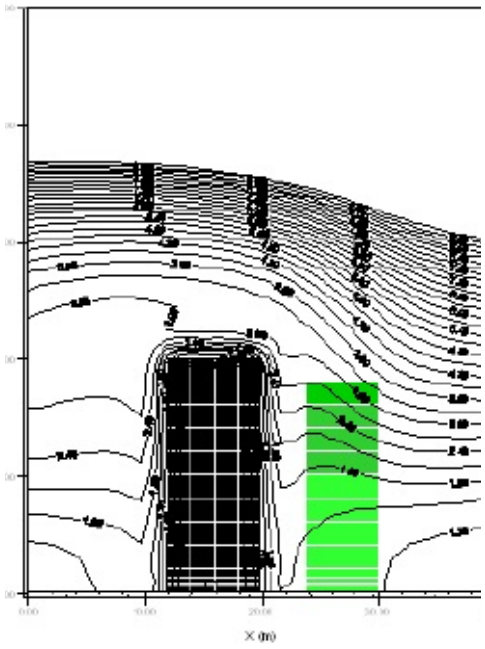

Km distribution for open LBC

low boundary is now more similar to the

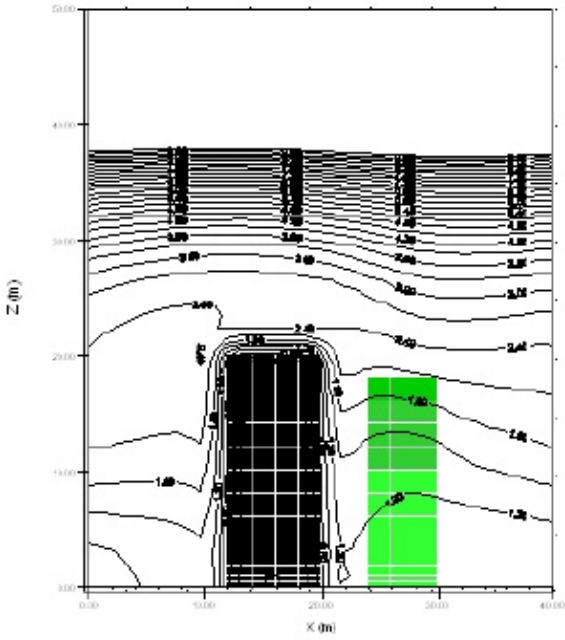

Km distribution for cyclic LBC

From Version 4 on, it is recomended to use at least the “Simple Forcing” option for temperature and humidity. This overcomes almost all problems that have been observed with the lateral boundaries in the former versions.

Instabilità – errori numerici

The problem...

In complex Model Areas (and sometimes even in configurations you consider as being "simple") you might experience numerical instabilities from time to time. ***These instabilities appear as "PANIC* Dumps"**

(if ENVI-met has detected that something went wrong) or simply as error messages or crushes of the model. The most frequent error message are "Division by Zero" or "Floating Point Error".

These messages do not contain any useful information except of the general message, that something went wrong. In fact, ***"Division by Zero" is most of the times only the end point of a long chain of problems producing very high or very low (and very wrong) numbers.***

Why is it like that...

First of all, remember that you are working with a very complex numerical model.

There is a conceptual difference between error messages you might get from, say, a text-processing program, and those you get from ENVI-met. Error messages (and the numerical problems which cause these messages) are inseperably connected with the whole process of numerical modelling.

If it would be possible to construct any Model Area and get guaranteed results, numerical modelling would no longer be an advanced technology ;). In other words: ***When you decide to use non-liner models like ENVI-met, you must be prepared that things are not always running as you would like them to run.*** Sometimes models run on the edge of numerical stability and a complex configuration might cause that they fall over this edge and send you an error message.

Running ENVI-met

The user friendly interface of ENVI-met sometimes makes people forget that they work with a sophisticated climate simulation system. Normally, these kind of numerical models can only be run on complex and extremely expensive supercomputers.

In more than 20 years of ENVI-met developement, we have invented various technologies to bring the scientific power of physical climate simulation models to your desktop. ENVI-met uses a complex system of optimized algorithms and intelligent troubleshooting allowing you to run dynamical 3D microclimate simulations on an arbitrary standard PC bought anywhere on the world running MS WINDOWS.

However, installing the software on your PC is the smallest step in using ENVI-met for microclimate analysis…

Database

Besides the two basic files needed for each simulation, the Area Input File .INX and the Simulation file .SIMX, ENVI-met needs to know a lot of additional information about different items used in your model such as surfaces types, soils, plants or emission sources in the model. These data are not stored in the Area Input file themself (exception: Packages), but in a database system.

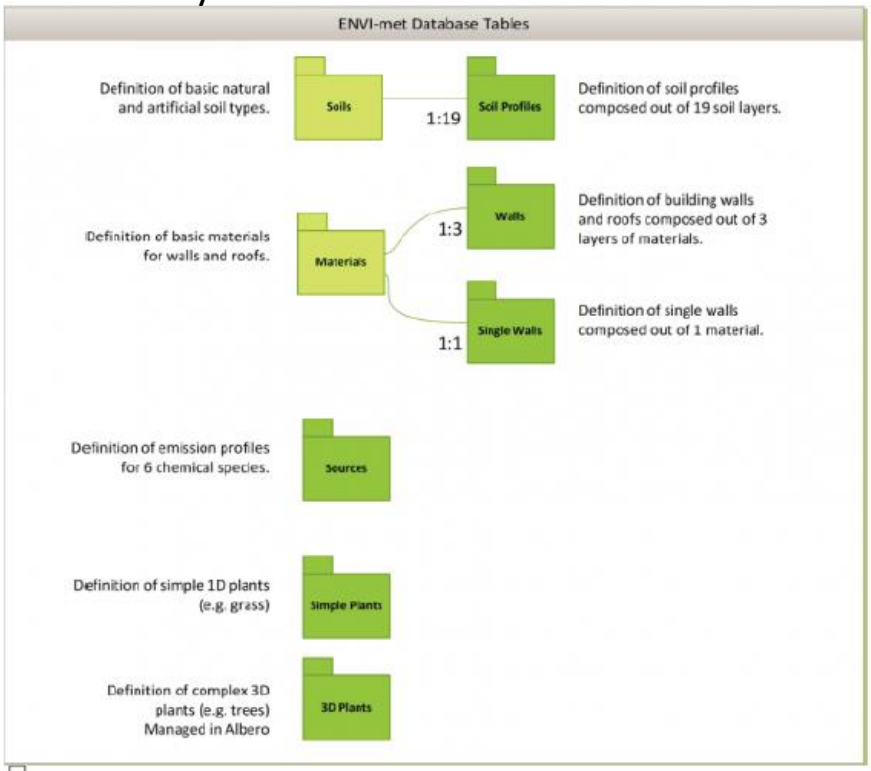

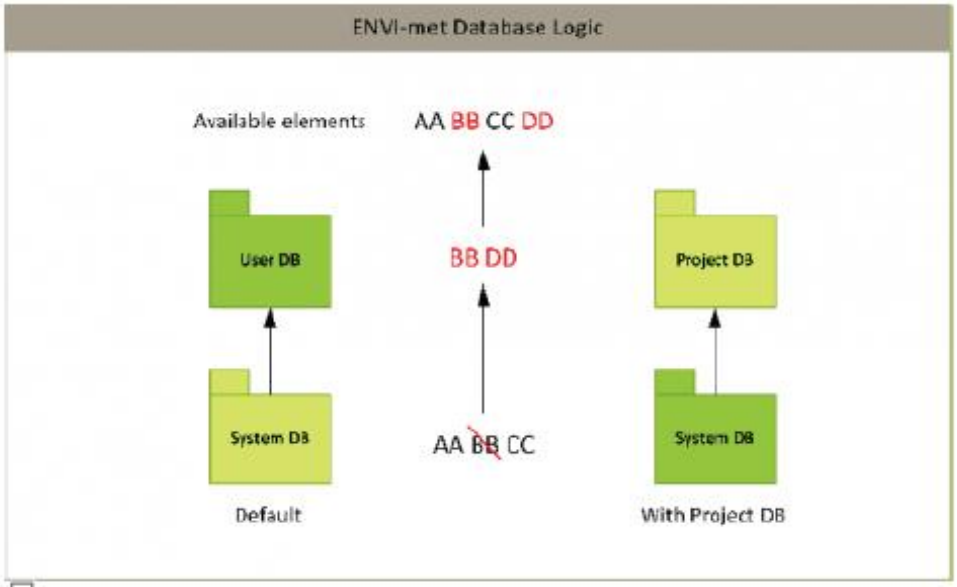

Logic of merging database items

Each database entry is defined by a unique key, which has to be a two-sign alphanumerical ID in ENVI-met (e.g. ”a0”). Any reference to a database entry, may it be in an Area Input file or some other table of the database is given by using this ID.

Il modello numerico 3D

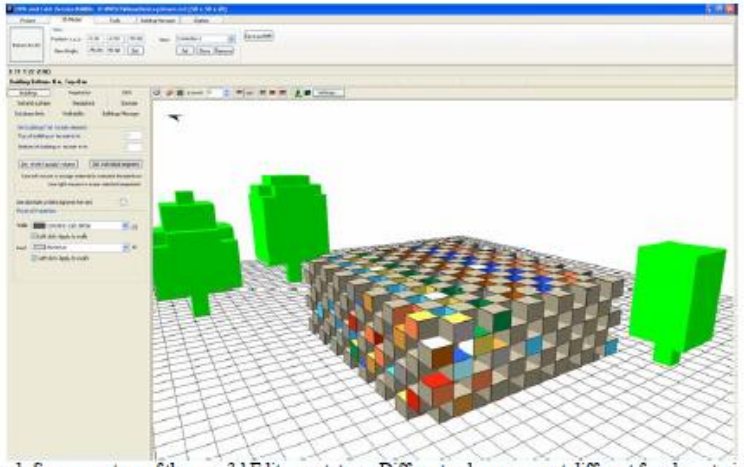

Fig. 1: Screen capture of the new 3d Editor prototype. Different colors represent different facade materials.

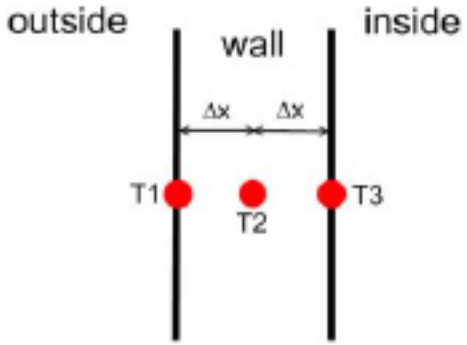

Fig. 2: Schematic of three node model

The energy balance of the outer façade surface can be written as

$$Q_{sw,net}^{abs} + Q_{lw,net}^{abs} - \varepsilon\sigma T_{1,2}^{4} + h_{c,o}(T_{air} - T_1^*) + \frac{\lambda}{\Delta x}(T_2^* - T_1^*) = \frac{c_{wall}\rho\Delta x}{2\Delta t}(T_1^* - T_1)$$

with $Q_{sw,net}^{abs}$ and $Q_{lw,net}^{abs}$ being the absorbed incoming short wave and long wave radiation [W], ε the emissivity [%], σ the Stefan-Boltzman constant, $h_{c,o}$ is the convection coefficient for the outside wall [W/(m²K)], λ the heat transfer coefficient [W/(mK)], Δx the distance between two nodes [m], c_{wall} heat capacity of the wall [J/(kgK)], $T_n^{(*)}$ the temperature at node n at present (T_n) or future (T_n^*) time step.

Il modello numerico 3D

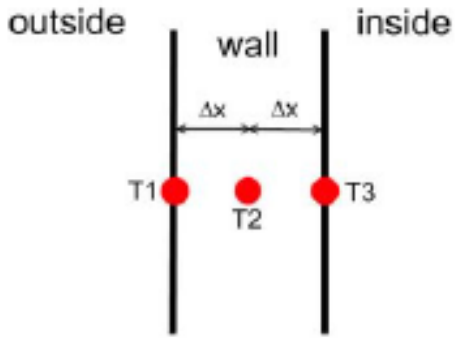

Fig. 2: Schematic of three node model

With the Fourier Equation

$$\frac{\delta T}{\delta t} = \frac{\lambda}{c_{wall}\rho}\frac{\delta^2 T}{\delta x^2}$$

the energy fluxes at the node in the center of the wall can be summed up as

$$(P+2)T_2^* - T_3^* = PT_2 + T_1^*$$

with $P = \frac{\Delta x^2 c_{wall}\rho}{\lambda \Delta t}$.

For the node at the inside of the wall the energy balance sums up to

$$-T_2^* + (\frac{P}{2} + \frac{h_c \Delta x}{\lambda} + 1)T_3^* = \frac{P}{2}T_3 + \frac{h_{c,i}\Delta x}{\lambda}T_i$$

with $h_{c,i}$ as the heat convection coefficient at the inside (7.7W/(m²K)).

Cosa si può modellare con ENVI-MET – Vegetazione e Alberature

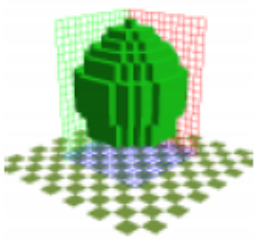

3D Plant Geometry

ENVI-met supports simple vertical plants such as grass or corn, but also allows complex 3D vegetation geometries like large trees. All plants are treated as individual species with an integrated water balance control and heat and water stress reaction concept.

Vegetation water supply

Plants are living organisms and will only contribute in positive way to the local microclimate, if enough water is available in the soil within the root zone. Together with the simulation of the soil water content and the new sophisticated 3D root model, the dynamic water supply of the plant and the resulting water extraction from the soil can be calculated.

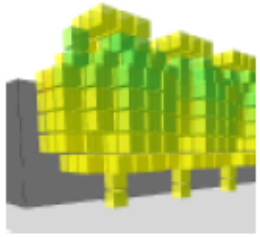

Foliage temperature

The temperature of the leafs is calculated by solving the energy balance of the leaf surface with respect to the actual meteorological and plant physiological conditions for each grid box of the plant canopy. The health status of the plant and the water supply by the soil regulate, beside other factors, the plants transpiration rate and thereby the leaf temperature. ENVI-met uses a sophisticated model to simulate the stomata behaviour of the vegetation in response to microclimate, CO2 availability and water stress level.

Cosa si può modellare con ENVI-MET – Edificio e involucro

Surface and soil temperature

The surface temperature and the distribution of soil temperature is calculated for natural soils and for artificial seal materials down to a depth of -4m. For each vertical grid layer a different soil or sealing material can be chosen in order to simulate different soils structures. The heat conductivity of natural soils is calculated with respect to the actual soil water content.

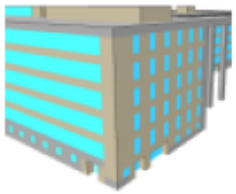

Detailed building materials

In Detailed Design Mode, ENVI-met allows to assign individual wall types to each wall and roof surface. The wall types can be composed out of 3 layers of different materials with individual physical properties such as solar radiation transmission, heat capacity or heat conductivity. The different wall and roof materials can be designed graphically using the Database Manager.

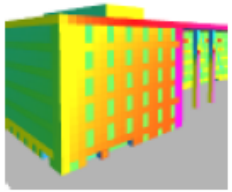

Each wall and roof segment in ENVI-met is represented by its own thermodynamical model consisting of 7 prognostic calculation nodes. The temperature of the outside node is updated continuously with respect to the meteorological variables at the facade and the thermal state of the buildings and other objects within the view range of the facade/roof element considered. The thermal state of the inner wall nodes is calculated from the physical properties assigned to the wall/roof based on Fourier's law of heat conduction

Full 3D building geometry & Single walls

Complex buildings and other structures can be constructed in full 3D with no limitations in complexity as far as the cubic base structure allows. This allows the simulation of semi-open spaces such as the soccer stadium shown in the icon and in this example. Moreover, ENVI-met Professional allows the usage of single thin walls that can be applied to any grid which can be used to represent spaces wich are enclosed by walls but do not behave like a building e.g. bus stop shelters, shading structures...

Cosa si può modellare con ENVI-MET – Situazioni specifiche

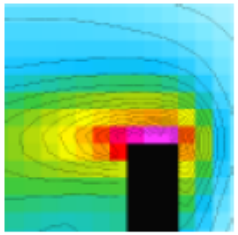

Turbulence

Turbulence is calculated using the E-epsilon 1.5order closure ("E-epsilon" or "k-epsilon" model). Two prognostic equations for turbulent energy production (E) and its dissipation (ϵ) are used to simulate the distribution of turbulent energy. Exchange coefficients (K_x) in the air are calculated using the Prandtl-Kolmogorov relation. For low wind situations, the 1st order mixing length model can be used instead of the E-epsilon model (which often fails in this situations).

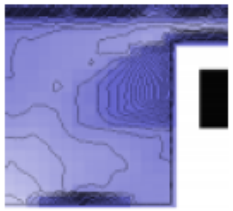

Soil water content

Simulating the water balance of the surface and the soil is a crucial aspect in urban microclimatology. While humid soils can act as cooling devices, dry soils are often hotter than asphalt. In addition, the cooling effect, and -on a longer time perspective- the vitality of vegetation depends on available soil water. ENVI-met dynamically solves the soil hydraulic state of the soil based on Darcy's law

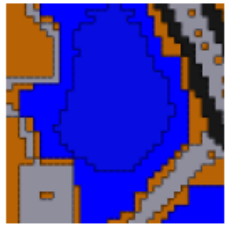

Water bodies and pounds

Water bodies are represented as a special type of soil. The calculated processes inside the water include the transmission and absorption of shortwave radiation inside the water. No second energy balance is used for the ground surface of the water pool, so that heating of shallow systems is lower than under real conditions where the main source of energy is the convection from the water ground surface rather than the absorption of radiation. In addition, no turbulent mixing is included in the model so that the use is restricted to still waters (e.g. lakes).

Modellazione del Comfort Outdoor
Interpretare i risultati: rassegna scientific literature

Kristian Fabbri - 29 Settembre 2017

Valutazione e proprietà dei materiali e morfologia urbana

Valutazione e proprietà dei materiali e morfologia urbana

Energy and Buildings 108 (2015) 156–174

Contents lists available at ScienceDirect

Energy and Buildings

journal homepage: www.elsevier.com/locate/enbuild

Microclimate development in open urban spaces: The influence of form and materials

Angeliki Chatzidimitriou [a,*], Simos Yannas [b]

[a] Aristotle University of Thessaloniki, School of Engineering, Thessaloniki, Greece
[b] Architectural Association Graduate School, London, UK

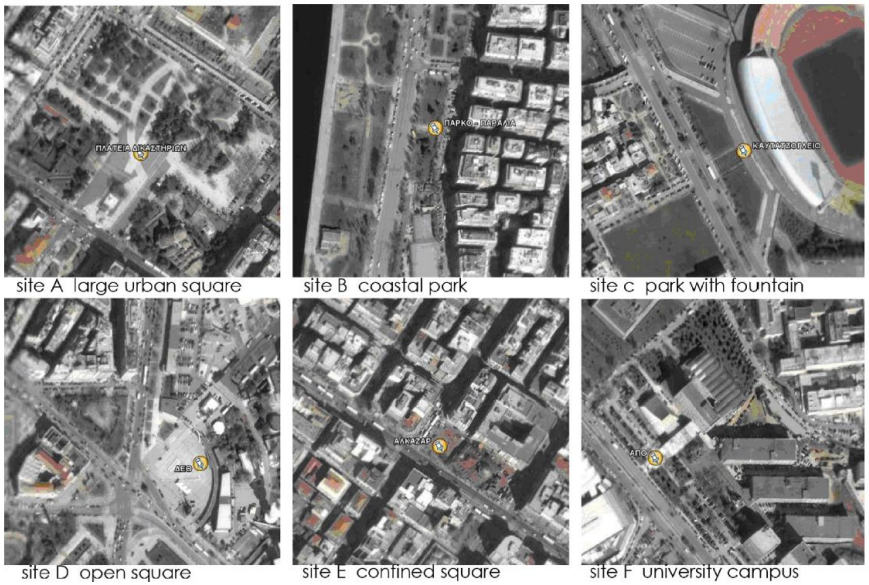

Table 1
Sky view factors at the locations of monitoring points in each site at 1 m above ground level and indicative values of solar radiation (direct and diffuse) and long-wave radiation at summer noon (calculated by ENVI-met v3 on specific days at 14:00).

Site| date | monitoring point	SVF	Solar radiation (W/m²)	Longwave radiation (W/m²)
Site A – large square | 29 July			
Marble black and white	0.90	998	3
Marble white and black	0.86	998	4
Cobble stone grey granite	0.89	998	3
Porous stone beige	0.86	998	4
Marble white	0.79	897	4
Grass	0.79	918	4
Grass (below tree shade)	0.20	109	4
Site B – coastal park | 26 August			
Concrete tiles	0.73	830	11
Grass	0.71	826	15
Concrete tiles (below tree)	0.32	561	29
Grass (below tree)	0.31	576	13
Concrete tiles (below tent)	0.16	320	40
Concrete tiles (below canopy)	0.11	288	75
Site C – park with fountain | 25 August			
Asphalt	0.77	748	39
Marble grey	0.87	779	10
Grass	0.87	780	9
Water	0.87	779	9
Site D – open square | 29 June			
Concrete and gravel white – grey	0.93	856	3
Site E – confined square | 29 June			
Ceramic tiles red	0.65	790	53
Site F – university campus | 03 August			
Asphalt	0.70	989	87
Marble white and grey	0.65	986	106
Concrete tiles	0.31	934	261
Brick red	0.30	933	265

Valutazione e proprietà dei materiali e morfologia urbana

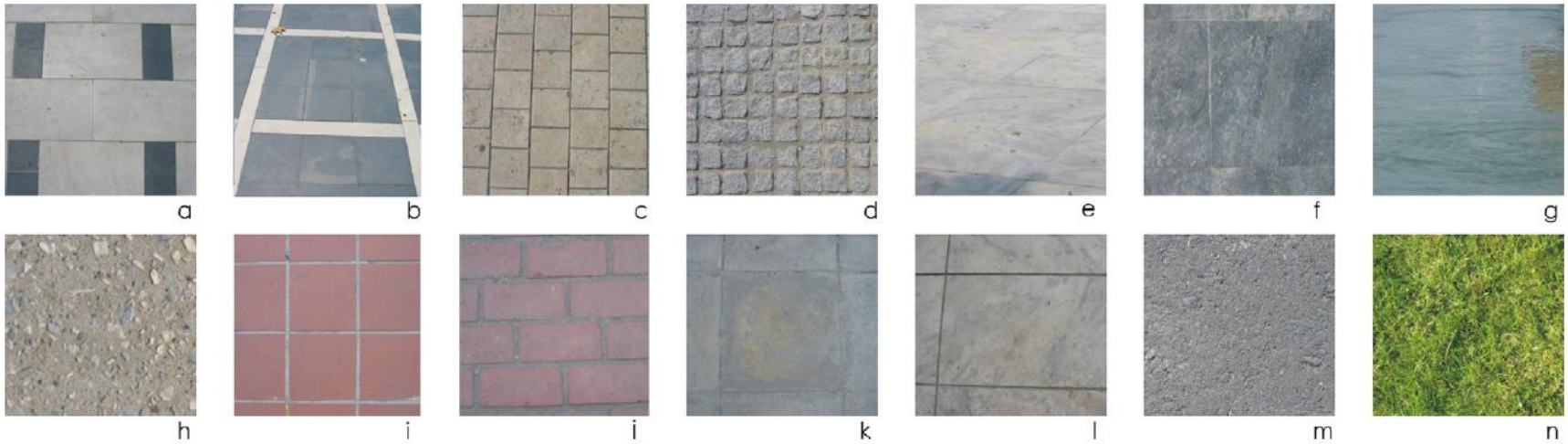

Fig. 2. Ground surface materials at the examined urban sites: (a) marble white (and black), (b) marble black (and white), (c) porous stone, (d) cobble stone by grey granite, (e) marble white (plain), (f) marble dark grey, (g) water surface (fountain), (h) concrete with gravel, (i) red ceramic tiles, (j) red bricks, (k) concrete tiles, (l) marble white (and grey), (m) asphalt and (n) grass. (For interpretation of the references to colour in this figure legend, the reader is referred to the web version of the article.)

Valutazione e proprietà dei materiali e morfologia urbana

Fig. 25. Views of the monitoring points at the university campus (site F): (a) marble white and grey, (b) asphalt, (c) concrete tiles in NW courtyard, (d) red bricks in central courtyard.

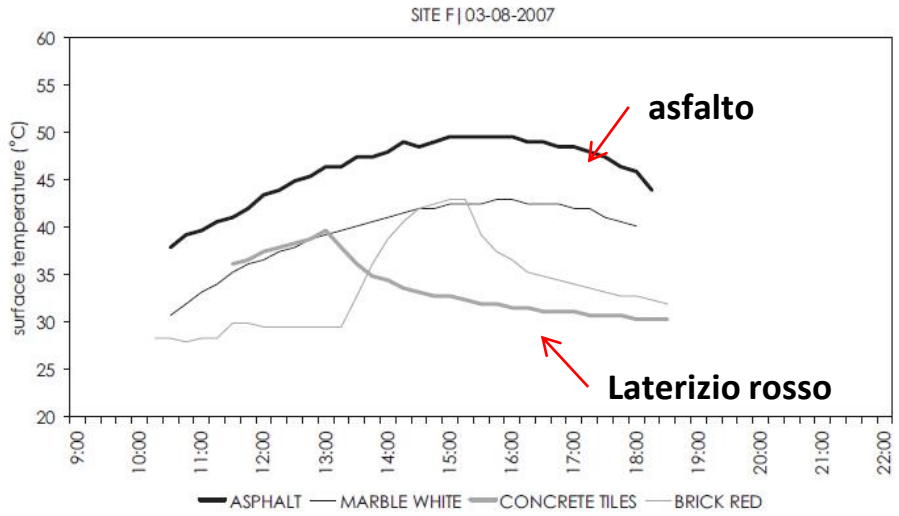

Fig. 26. Ground surface temperatures at the university campus (site F) on 03-08-2007.

Fig. 12. Monitoring spots at the coastal park at site b: (a) concrete tiles exposed, (b) grass exposed, (c) grass below tree shade, (d) concrete tiles below tree shade, (e) fabric tent shading concrete tiles and (f) timber gallery shading concrete tiles.

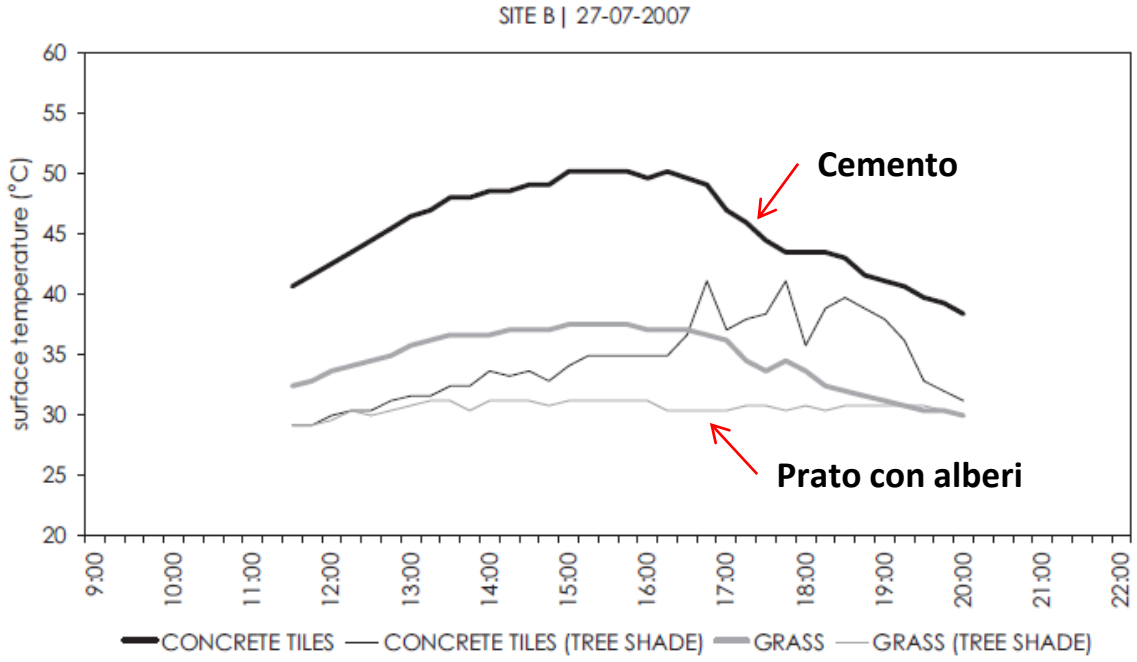

Fig. 13. Ground surface temperatures at the coastal park (site B) on 27-07-2007.

Valutazione e proprietà dei materiali e morfologia urbana

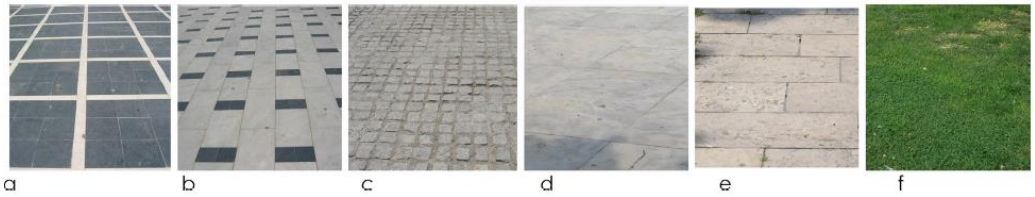

Fig. 6. Ground surface materials at site A: (a) marble black and white, (b) marble white and black, (c) granite cobble stones grey, (d) marble all-white, (e) porous stone beige and (f) Grass.

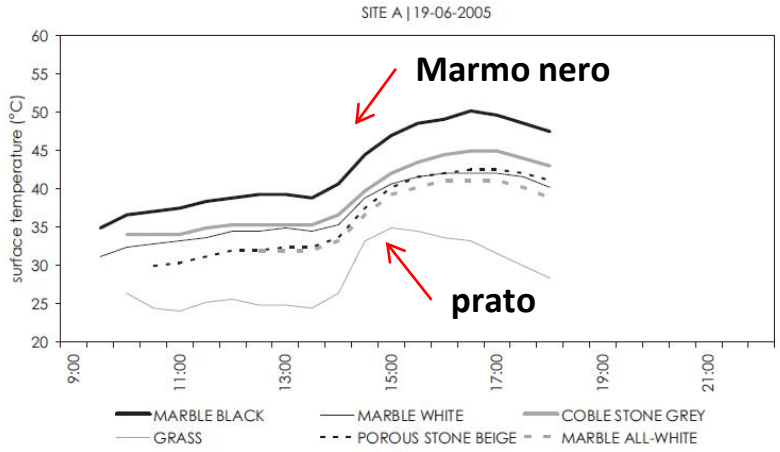

Fig. 7. Ground surface temperatures at the large square (site A) on 19-06-2005.

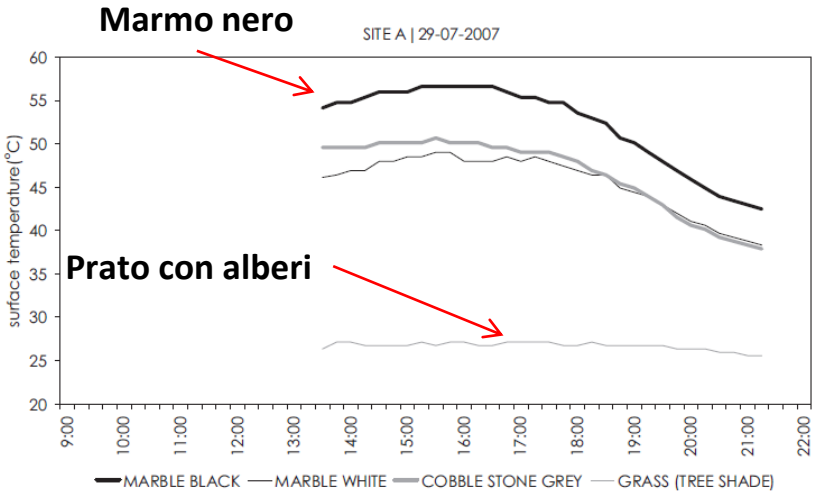

Fig. 8. Ground surface temperatures at the large square (site A) on 29-07-2007.

Morfologia urbana

Landscape and Urban Planning 125 (2014) 146–155

Contents lists available at ScienceDirect

Landscape and Urban Planning

journal homepage: www.elsevier.com/locate/landurbplan

Research Paper

Application of Universal Thermal Climate Index (UTCI) for microclimatic analysis in urban thermal environme

Sookuk Park[a,*], Stanton E. Tuller[b], Myunghee Jo[c]

[a] Horticultural Science, College of Applied Life Science, Jeju National University, 102 Jejudaehakno, Jeju-si, Jeju Special Self-Governing Province, 690-756, Republic of Korea
[b] Department of Geography, University of Victoria, Victoria, BC, Canada
[c] School of Convergence and Fusion system Engineering, Kyungpook National University, Republic of Korea

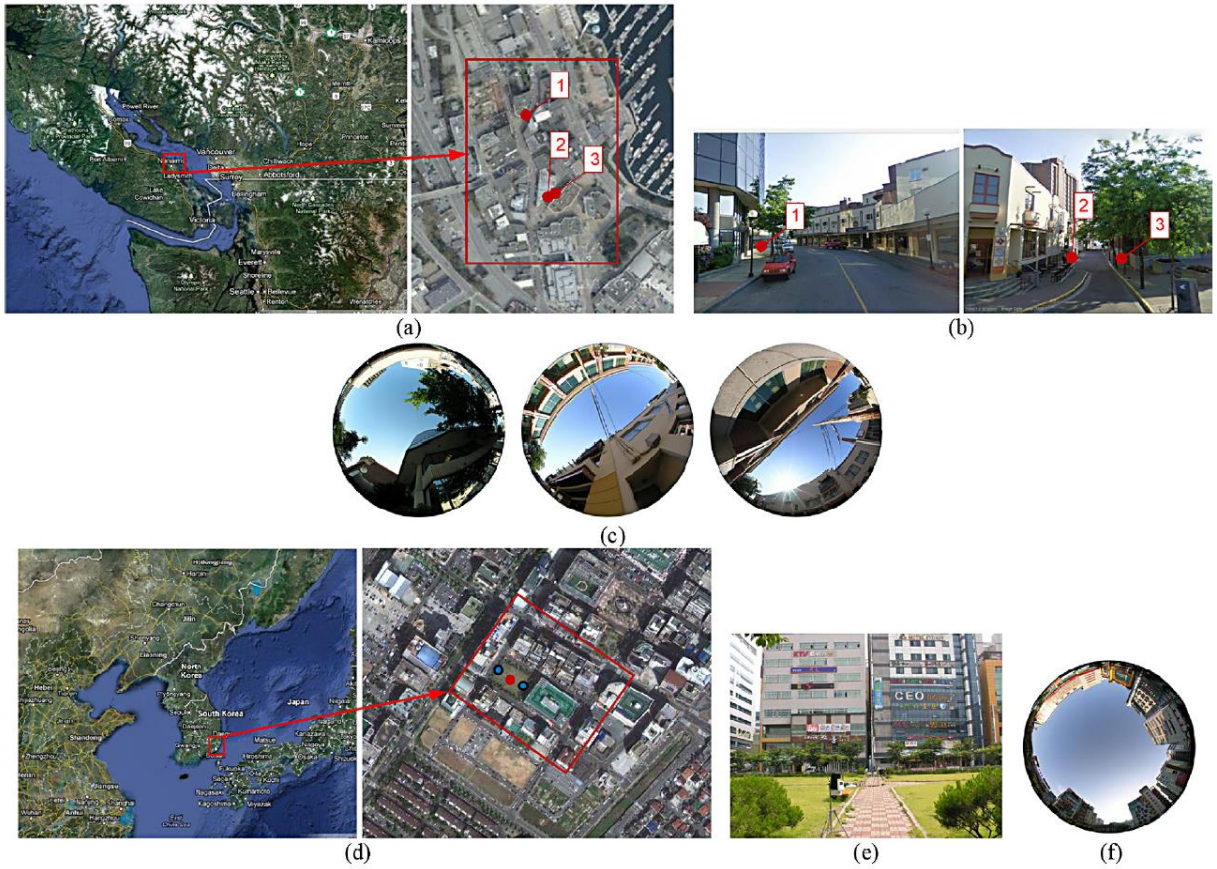

Fig. 1. Study locations: (a) Nanaimo location from Google map (http://maps.google.com), (b) street photographs of the Nanaimo sites (left, Nanaimo_1; right, Nanaimo_2 and 3), (c) fisheye lens photographs of the Nanaimo sites (left, Nanaimo_1, sky view factor (SVF) = 0.427; center, Nanaimo_2, SVF = 0.408; right, Nanaimo_3, SVF = 0.349) (Park, 2011, 2012), (d) Changwon location from Google map. Dots are site locations, (e) street photograph of the Changwon site, and (f) fisheye lens photograph of the Changwon site (SVF = 0.785) (Park, 2011, 2012). Fisheye lens photographs were taken using a Nikon Coolpix 8800 camera with Nikon FC-E9 fisheye converter lens and Nikon UR-E18 converter adapter. The collected ψ_{sky} values were determined using the BMSky-view computer program (Gál, Rzepa, Gromek, & Unger, 2007).

Morfologia urbana

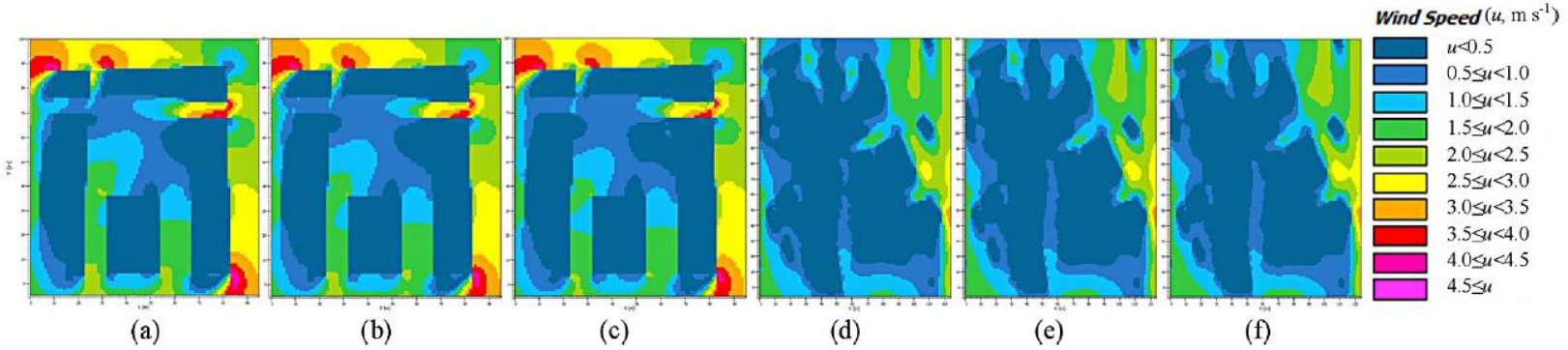

Fig. 5. ENVI-met wind speeds at (a) 11:30, (b) 14:00 and (c) 16:30 of Changwon and (d) 9:30, (e) 13:00 and (f) 16:30 of Nanaimo.

Table 4
Wind speed data at the Nanaimo sites.

July 26, 2009	Sites	Time	Measured wind speed ($m\,s^{-1}$)	ENVI-met wind speed ($m\,s^{-1}$)	Difference ($m\,s^{-1}$)
Morning	2	9:37	0.40	0.01	−0.39
	3	9:45	0.70	0.04	−0.66
	3	10:12	0.60	0.04	−0.56
	2	10:20	0.70	0.01	−0.69
	1	10:44	1.00	0.48	−0.52
	Mean				−0.56 ± 0.12
Noon	1	12:08	1.00	0.46	−0.54
	2	12:34	0.50	0.00	−0.50
	3	13:17	0.30	0.03	−0.27
	2	13:23	0.60	0.00	−0.60
	1	13:43	1.00	0.41	−0.59
	Mean				−0.50 ± 0.13
Afternoon	1	14:54	1.00	0.40	−0.60
	2	15:18	0.30	0.00	−0.30
	3	15:28	0.40	0.03	−0.37
	3	15:46	0.70	0.03	−0.67
	2	15:53	0.80	0.00	−0.80
	1	16:11	0.60	0.38	−0.22
	Mean				−0.49 ± 0.23

Morfologia urbana e materiali

Sustainable Cities and Society 14 (2014) 323–333

Contents lists available at ScienceDirect

Sustainable Cities and Society

journal homepage: www.elsevier.com/locate/scs

Urban gardens as a solution to energy poverty and urban heat island

Vasiliki Tsilini*, Sotiris Papantoniou, Dionysia-Denia Kolokotsa, Efpraxia-Aithra Maria

Technical University of Crete, School of Environmental Engineering, Crete, Greece

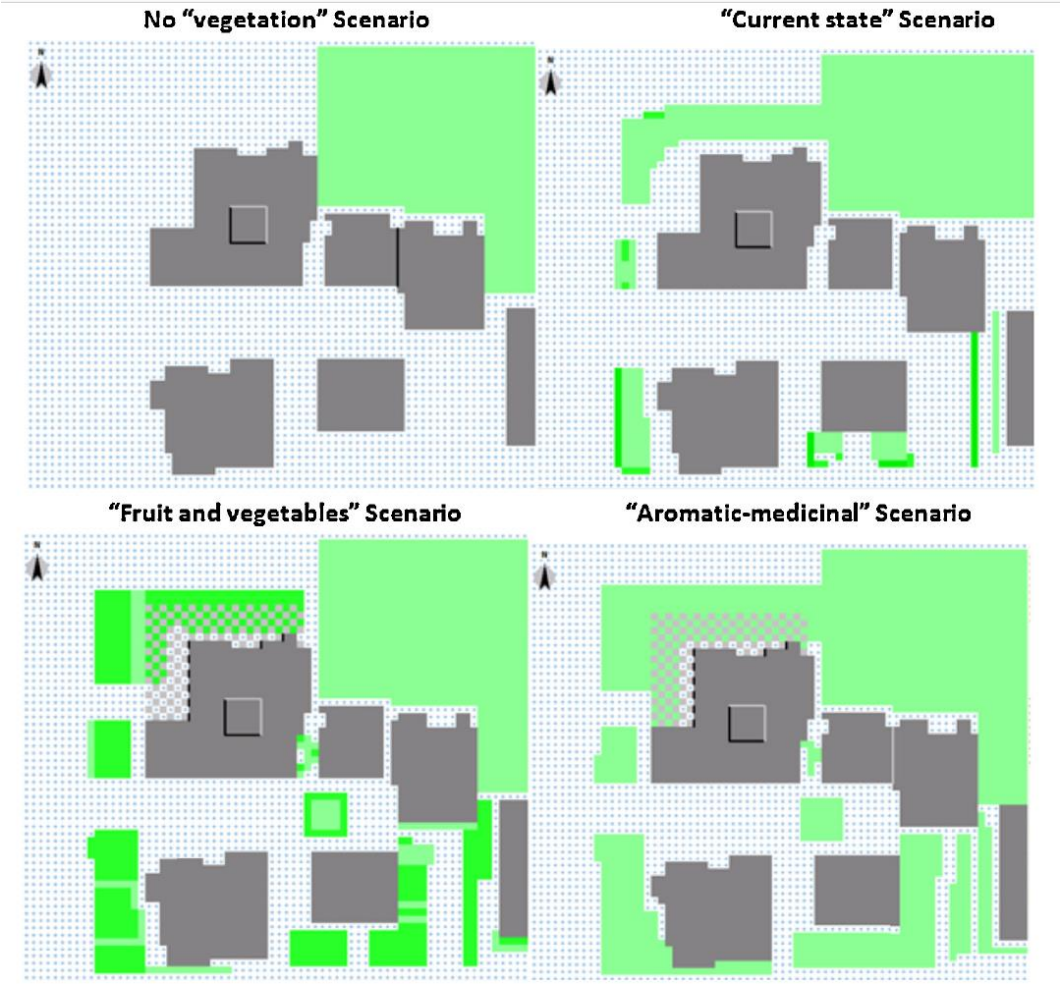

Fig. 3. Study area using Envi-met in each scenario.

Morfologia urbana e materiali

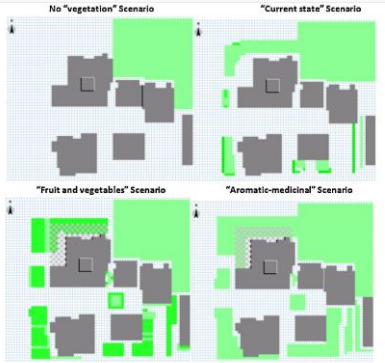

Fig. 3. Study area using Envi-met in each scenario.

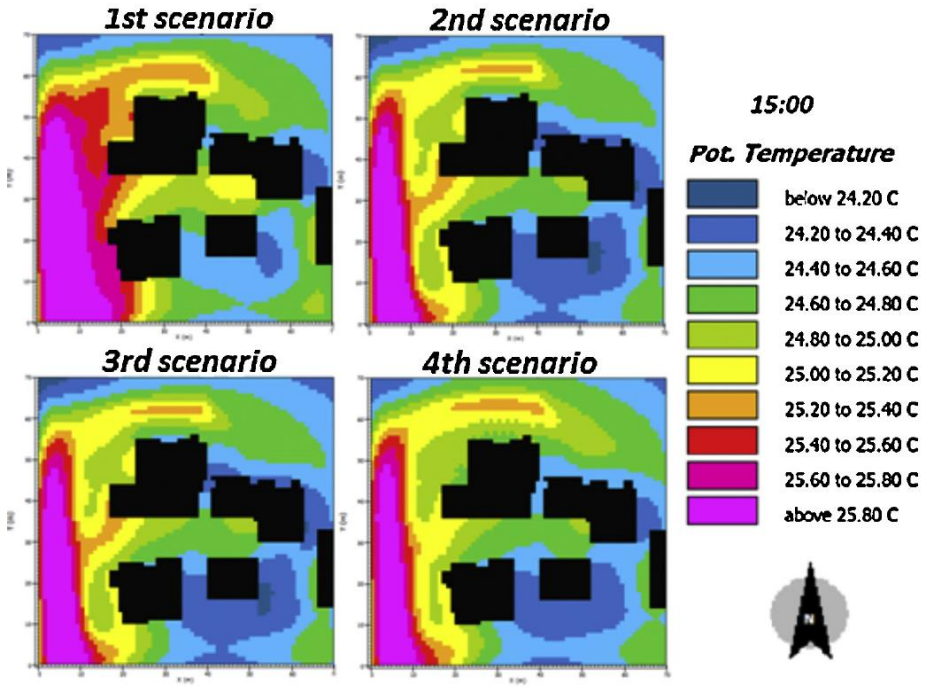

Fig. 4. Summer air temperature at 15 pm.

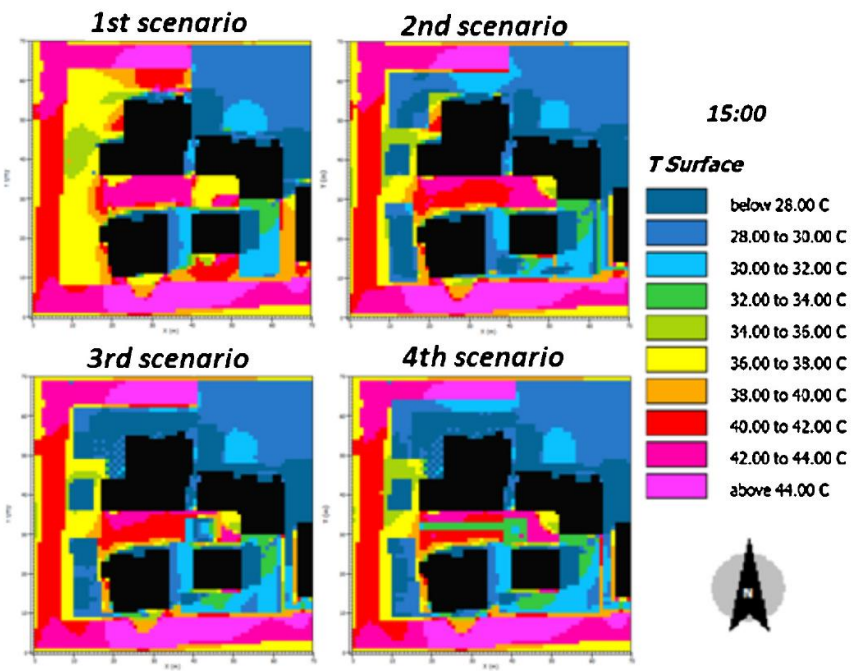

Fig. 5. Summer surface temperature at 15 pm.

Morfologia urbana - Canyon

Urban Climate 14 (2015) 251–267

Contents lists available at ScienceDirect

Urban Climate

journal homepage: www.elsevier.com/locate/uclim

Comparative analysis of green actions to improve outdoor thermal comfort inside typical urban street canyons

Gabriele Lobaccaro [a,*], Juan A. Acero [b]

[a] NTNU Norwegian University of Science and Technology, Department of Architectural Design, History and Technology, NO-7491 Trondheim, Norway
[b] TECNALIA, Energy and Environmental Division, Parque Tecnologico de Bizkaia, Edificio 700, 48160 Derio, Bizkaia, Spain

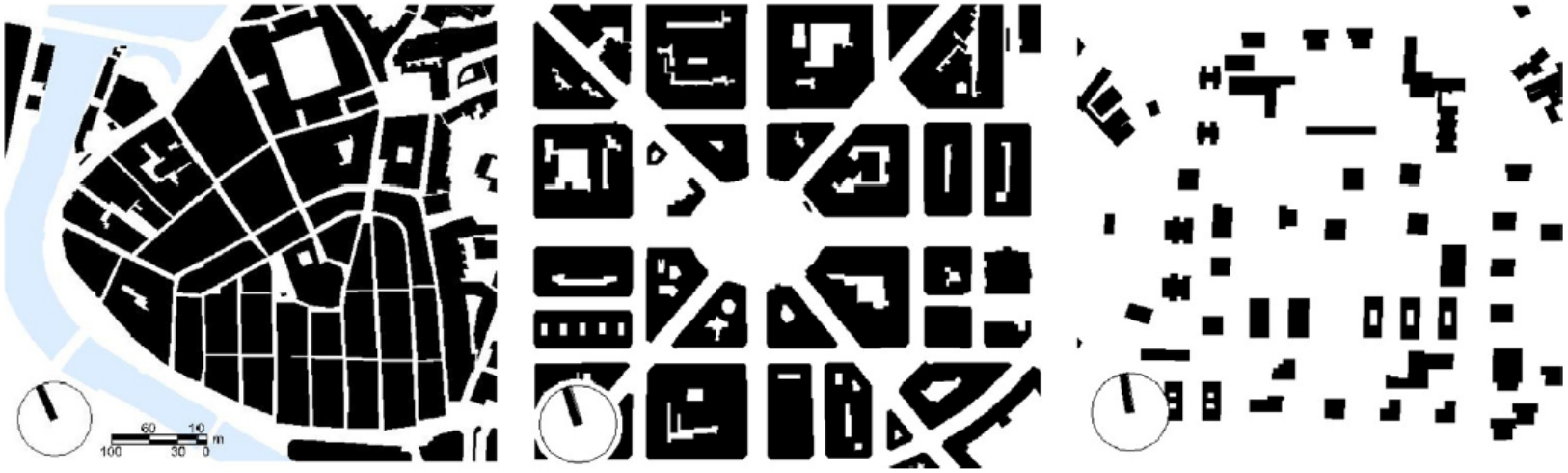

Fig. 1. Analysis of the empty and built spaces of the selected urban areas. From the left: *Casco Viejo*, *Abando/Indautxu* and the *Txurdinaga*.

Morfologia urbana - Canyon

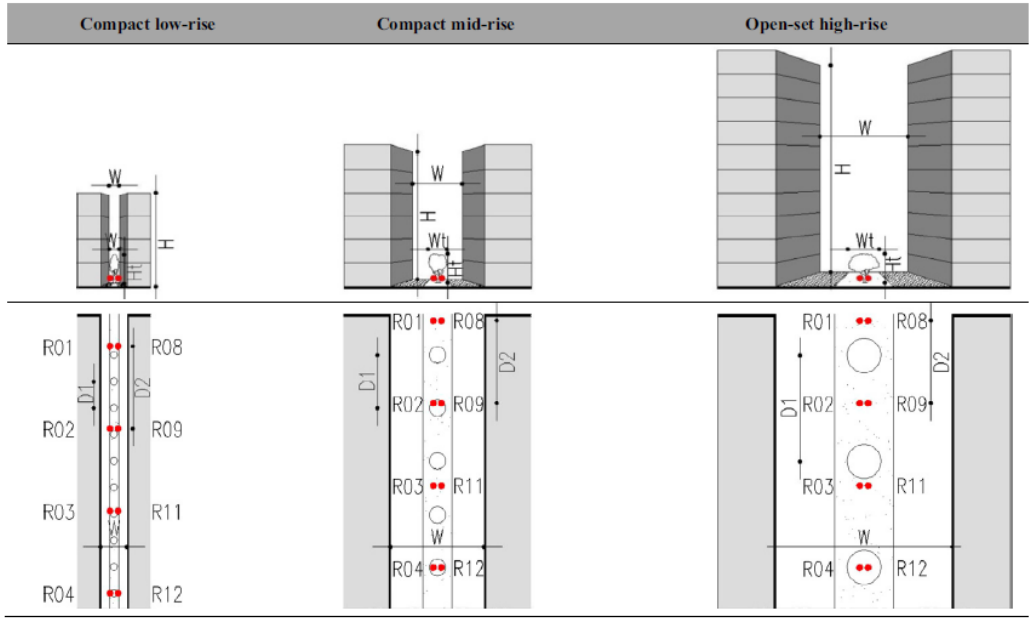

Fig. 3. The analyzed urban canyons with the position of the receptors, location of trees, distance between the trees (D_1), distance between the receptors (D_2) and foliage coverage of the trees. H/W = 3.5 Compact low-rise, H/W = 1.5 Compact mid-rise, H/W = 1.3 Open-set high-rise.

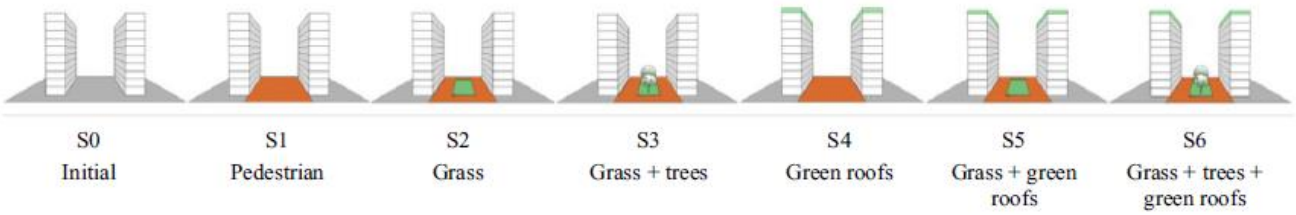

Fig. 4. The seven scenarios and the green actions analyzed in this work.

Morfologia urbana - Canyon

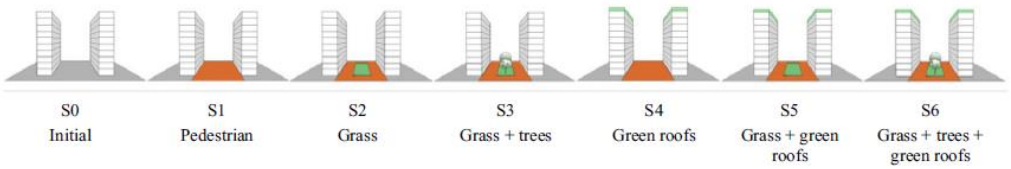

Fig. 4. The seven scenarios and the green actions analyzed in this work.

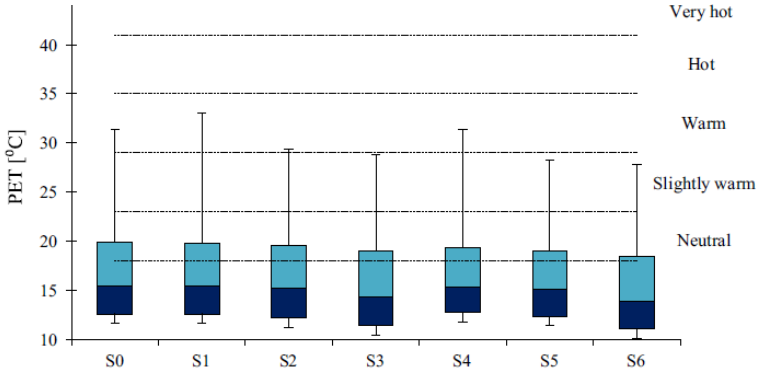

Fig. 5. The values of PET measured in all 14 receptors within the urban canyon in all the scenarios of open-set high-rise urban areas. Each box collects all the PET data recorded during the simulation day (7th of August): the bottom square, in dark blue, represents the 2nd or lower quartile (Q2) that is equal to 25% of the distribution of the all data under the average value of PET; the top square, in clear blue, is the 3rd or upper quartile (Q3) with the 25% of the data over the average value of PET; the average value marks the mid-point of the PET data and is shown by the line that divides the box into two parts. Half of the PET values, distributed in Q2, are greater than or equal to this value and half, distributed in Q3, are less. The upper (Q4) and lower (Q1) whiskers represent the distribution of the values outside the middle 50%. The whiskers also underline the outliers (extreme values). The upper whisker represents the peak of PET value recorded in each scenario. (For interpretation of the references to color in this figure legend, the reader is referred to the web version of this article.)

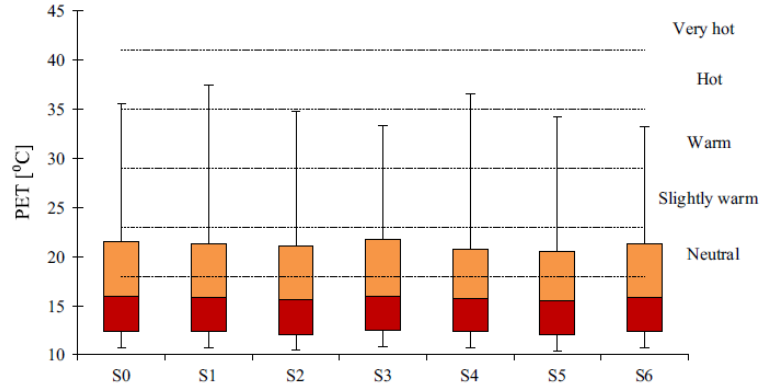

Morfologia urbana - Canyon

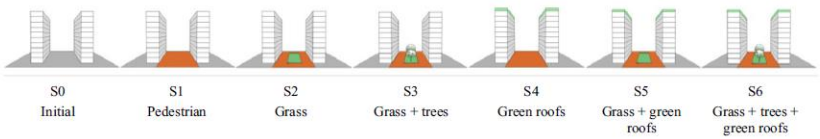

Fig. 4. The seven scenarios and the green actions analyzed in this work.

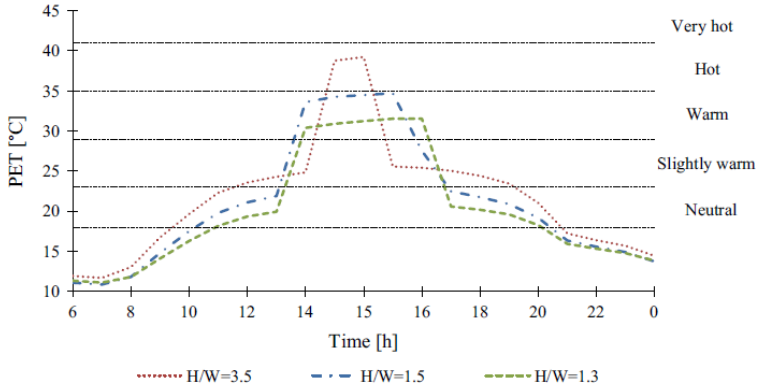

Fig. 8. The hourly evolution of the average peak values of PET calculated from the peak values of PET recorded from all 14 receptors within the urban canyon for scenario S1. The hourly evolution of PET for the different ratio of height (H) and width (W) have been represented: $H/W = 3.5$ for compact low-rise, $H/W = 1.5$ for compact mid-rise and $H/W = 1.3$ for open-set high-rise.

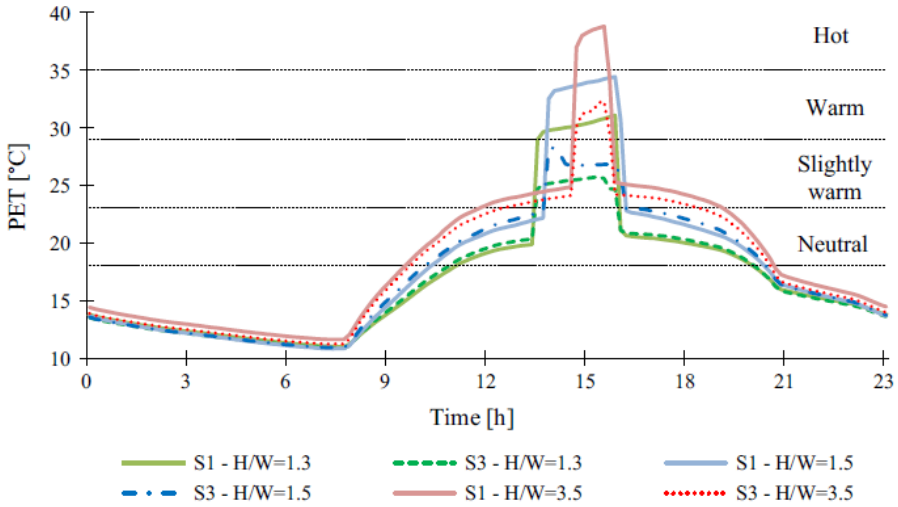

Fig. 14. Comparison of typical PET trends between scenario S1 and S3. Data related to receptor R04. The hourly evolution of PET for $H/W = 3.5$ for compact low-rise, $H/W = 1.5$ for compact mid-rise and $H/W = 1.3$ for open set high-rise have been represented.

Morfologia urbana - Canyon

Urban Climate 14 (2015) 251–267

Contents lists available at ScienceDirect

Urban Climate

journal homepage: www.elsevier.com/locate/uclim

Comparative analysis of green actions to improve outdoor thermal comfort inside typical urban street canyons

Gabriele Lobaccaro [a,*], Juan A. Acero [b]

[a] NTNU Norwegian University of Science and Technology, Department of Architectural Design, History and Technology, NO-7491 Trondheim, Norway
[b] TECNALIA, Energy and Environmental Division, Parque Tecnologico de Bizkaia, Edificio 700, 48160 Derio, Bizkaia, Spain

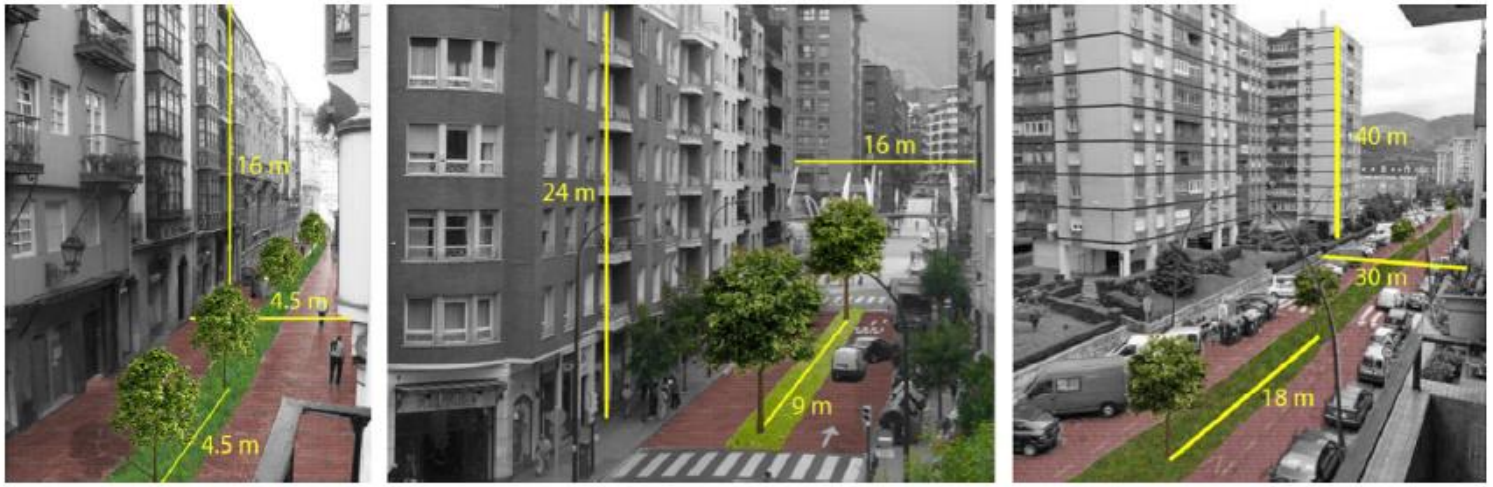

Fig. 16. (From left) Visualization of the green action in compact low-rise, compact mid-rise and open-set high-rise urban areas. (For interpretation of the references to color in this figure legend, the reader is referred to the web version of this article.)

Morfologia urbana

Sustainable Cities and Society 26 (2016) 27–47

Contents lists available at ScienceDirect

Sustainable Cities and Society

journal homepage: www.elsevier.com/locate/scs

Microclimate design for open spaces: Ranking urban design effects on pedestrian thermal comfort in summer

Angeliki Chatzidimitriou [a,*], Simos Yannas [b]

[a] Aristotle University of Thessaloniki, Faculty of Engineering, Thessaloniki, Greece
[b] Architectural Association Graduate School, London, UK

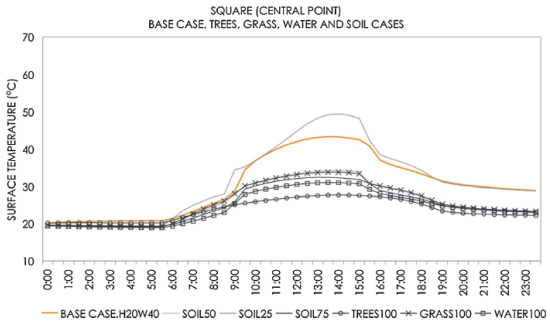

Fig. 12. Comparative diagram of hourly surface temperatures at the central point of the square in the cases of pavement (BASECASE.H20W40), natural soil with relative humidity 50%, 25% and 75% (SOIL50, SOIL 25 and SOIL75, respectively), full cover by trees, grass and water surfaces (TREES100, GRASS100 and WATER100, respectively): simulation results by ENVI-met software.

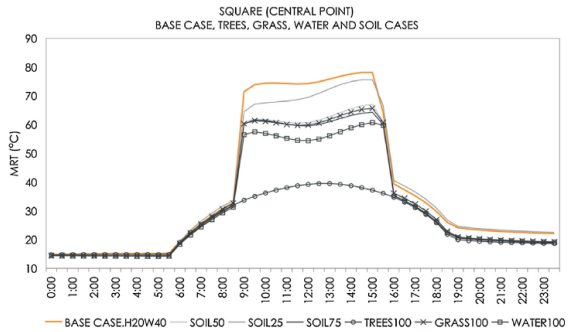

Fig. 13. Comparative diagram of hourly mean radiant temperatures at the central point of the square in the cases of pavement (BASECASE.H20W40), natural soil with relative humidity 50%, 25% and 75% (SOIL50, SOIL 25 and SOIL75 respectively), full cover by trees, grass and water surfaces (TREES100, GRASS100 and WATER100 respectively): simulation results by ENVI-met software.

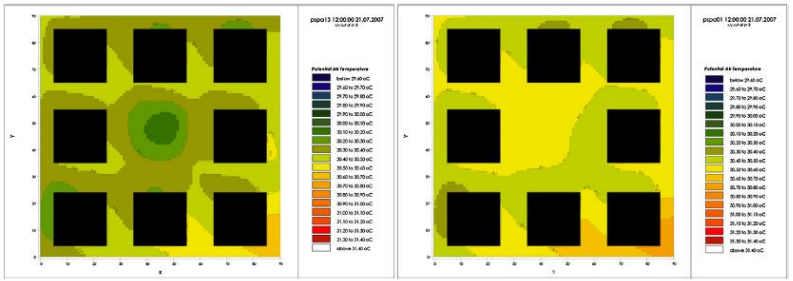

Fig. 9. Simulation results for air temperature at noon (1200 h), in the square, 1 m above ground level, in (a) the base case and (b) the case of 100% cover by trees (simulation results by ENVI-met).

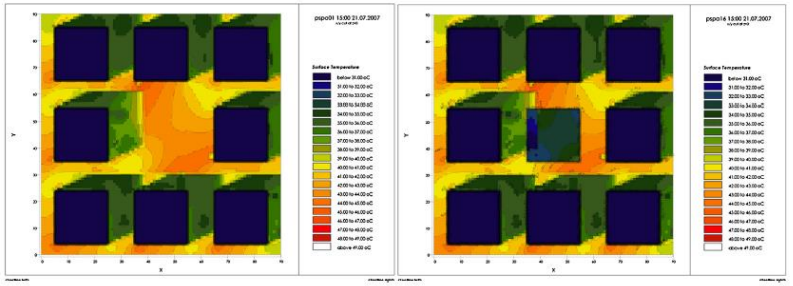

Fig. 10. Simulation results for ground surface temperature in the afternoon (1500 h), at the square, in (a) the base case and (b) the case of 100% cover by grass (simulation results by ENVI-met).

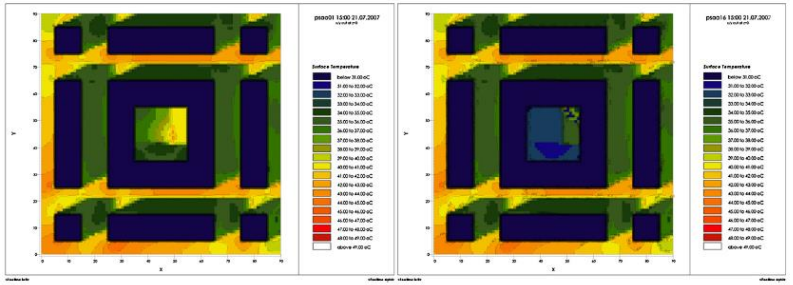

Fig. 11. Simulation results for ground surface temperature in the afternoon (1500 h), at the courtyard, in (a) the base case and (b) the case of 100% cover by grass (simulation results by ENVI-met).

Morfologia urbana

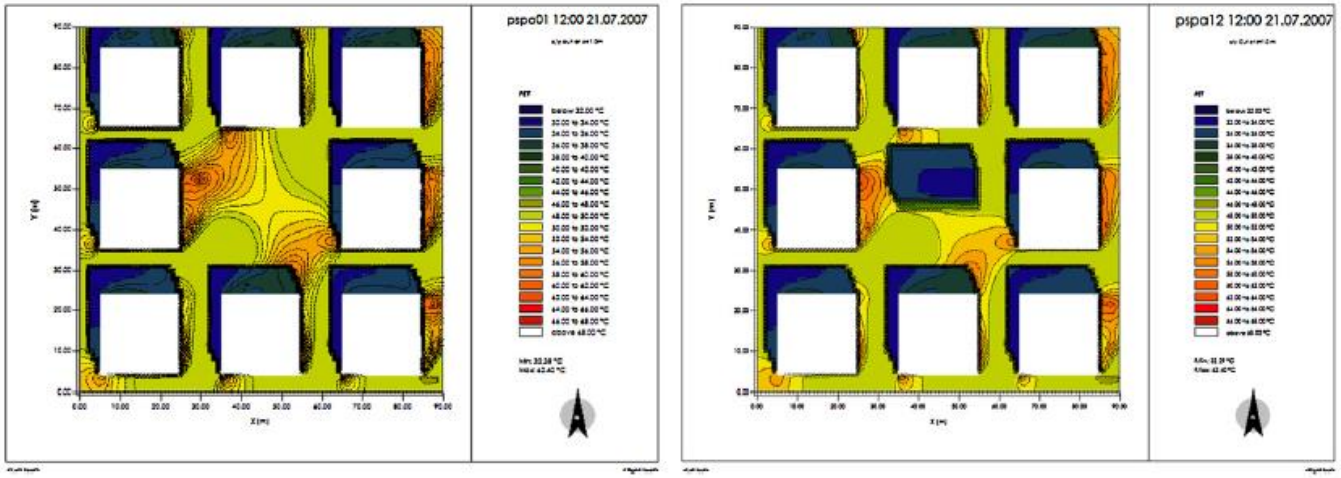

Fig. 18. PET values at noon in the square 1 m above ground level, in (a) the base case and (b) the case of 50% cover by trees.

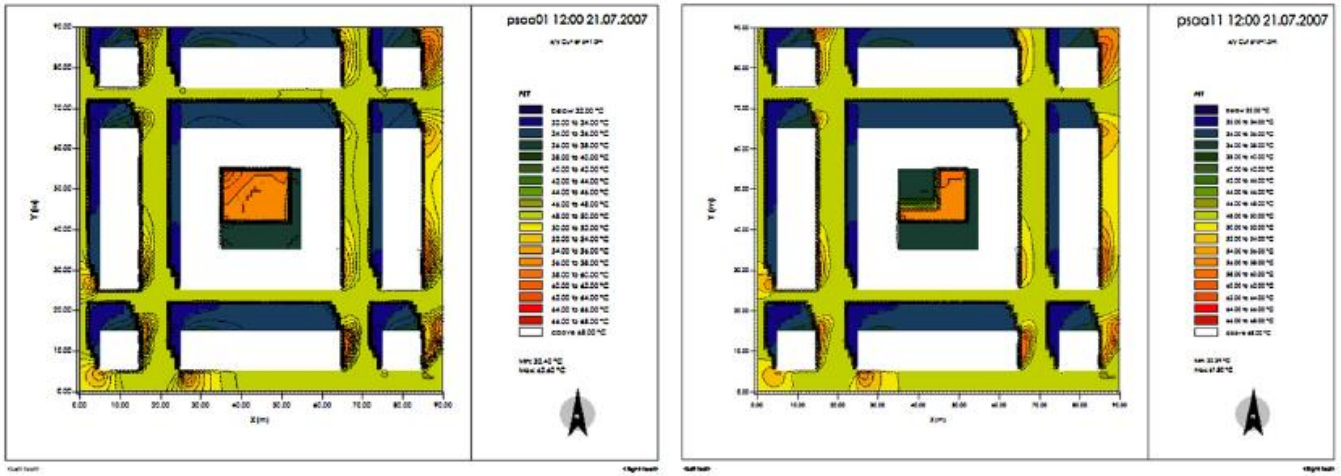

Fig. 19. PET values at noon in the courtyard 1 m above ground level, in (a) the base case and (b) the case of 25% cover by trees.

Building and Environment 60 (2013) 93–104

Contents lists available at SciVerse ScienceDirect

Building and Environment

journal homepage: www.elsevier.com/locate/buildenv

Evaluation of a microclimate model for predicting the thermal behavior of different ground surfaces

Xiaoshan Yang [a,b], Lihua Zhao [a,*], Michael Bruse [b], Qinglin Meng [a]

[a] Building Environment and Energy Laboratory (BEEL), State Key Laboratory of Subtropical Building Science, South China University of Technology, Wushan Road 381, Guangzhou, China

[b] Environmental Modelling Group (EMG), Johannes Gutenberg-Universität Mainz, Mainz, Germany

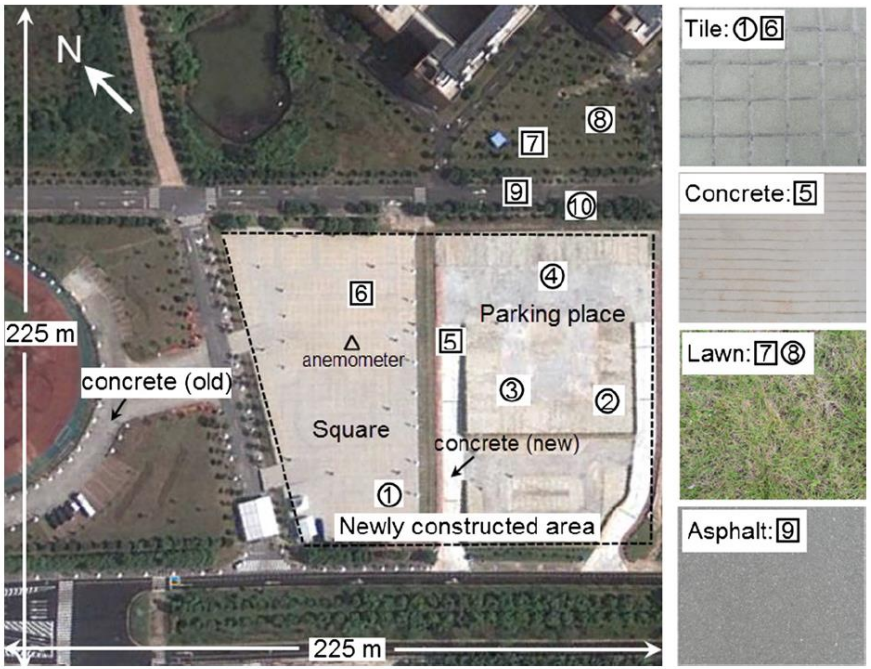

Fig. 1. Experimental area (image is from Google Earth), the layout of measurement points, and the features of the studied ground surfaces (right). For points 5, 6 and 7, both sub- and above-surface variables were measured. For point 9, only the above-surface variables were observed. For points 1, 2, 3, 4, 8 and 10, only air temperature and relative humidity at 0.2 m and 1.5 m above ground were measured. The anemometer sensor was located in the center of the square, 2 m above ground.

Morfologia urbana Canyon

ELSEVIER

Available online at www.sciencedirect.com
ScienceDirect
Solar Energy 81 (2007) 742–754

SOLAR ENERGY
www.elsevier.com/locate/solener

Effects of asymmetry, galleries, overhanging façades and vegetation on thermal comfort in urban street canyons

Fazia Ali-Toudert *, Helmut Mayer

Meteorological Institute, University of Freiburg, Werderring 10, 79110 Freiburg, Germany

Received 29 December 2005; received in revised form 9 October 2006; accepted 10 October 2006
Available online 15 November 2006

Communicated by: Associate Editor Mattaios Santamouris

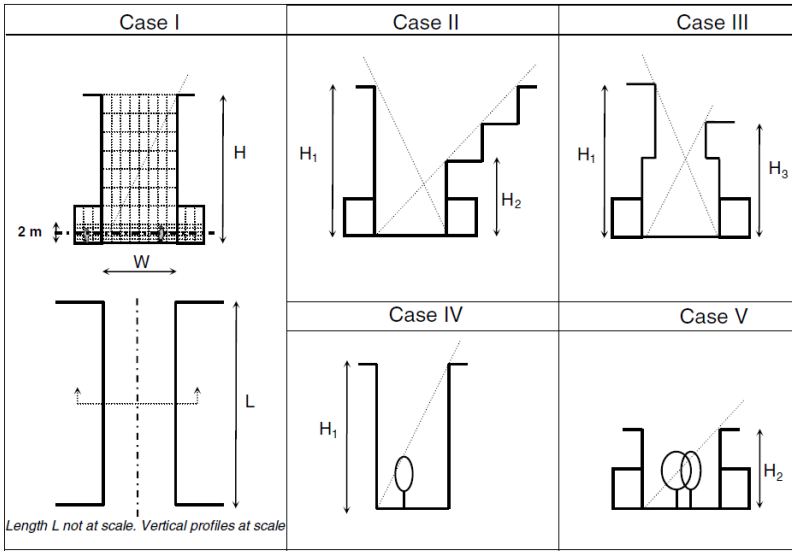

Fig. 1. Urban canyon geometries used in the simulations with ENVI-met 3.0.

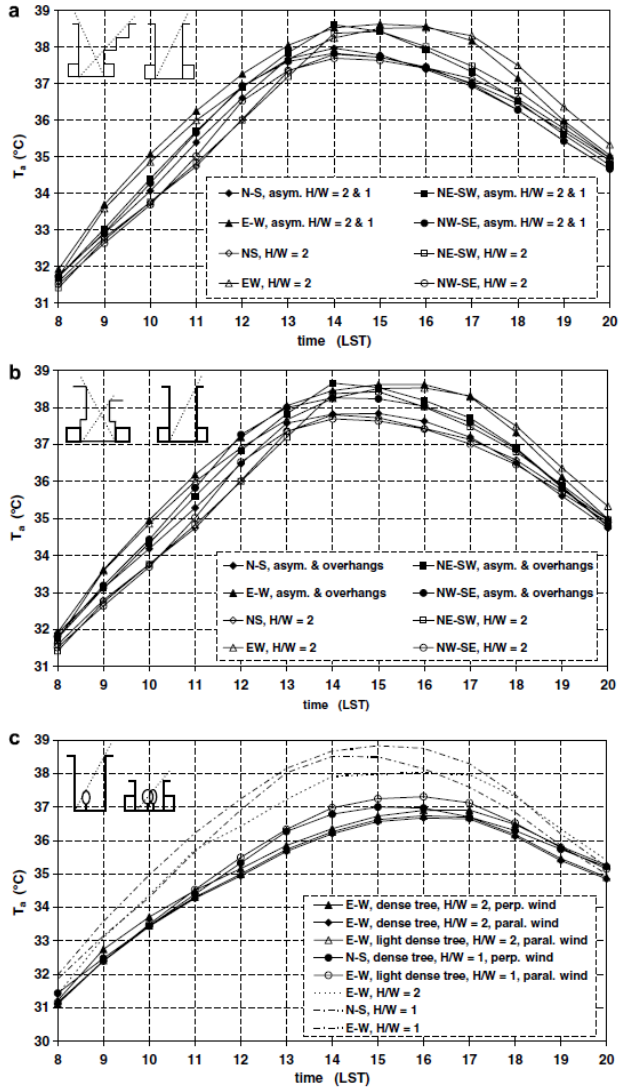

Fig. 2. Average air temperature T_a at street level (1.2 m a.g.l.) for (a) asymmetrical urban canyons, (b) overhanging façades, and (c) urban canyons with trees, in comparison to symmetrical urban canyons of $H/W = 2$ and 1.

OMM Outdoor Microclimate Map

Available online at www.sciencedirect.com

ScienceDirect

Energy Procedia 111 (2017) 510 – 519

Energy Procedia

8th International Conference on Sustainability in Energy and Buildings, SEB-16, 11-13 September 2016, Turin, ITALY

Outdoor Comfort: the ENVI-BUG tool to evaluate PMV values Output Comfort point by point

Kristian Fabbri[a], Antonello Di Nunzio[a], Jacopo Gaspari[a]*, Ernesto Antonini[a], Andrea Boeri[a]

[a]*Department of Architecture, University of Bologna, viale Risorgimento 2, Bologna 40136, Italy*

OMM Outdoor Microclimate Map

Available online at www.sciencedirect.com
ScienceDirect
Energy Procedia 111 (2017) 510 – 519
Energy Procedia
ELSEVIER

8th International Conference on Sustainability in Energy and Buildings, SEB-16, 11-13 September 2016, Turin, ITALY

Outdoor Comfort: the ENVI-BUG tool to evaluate PMV values Output Comfort point by point

Kristian Fabbri[a], Antonello Di Nunzio[a], Jacopo Gaspari[a]*, Ernesto Antonini[a], Andrea Boe

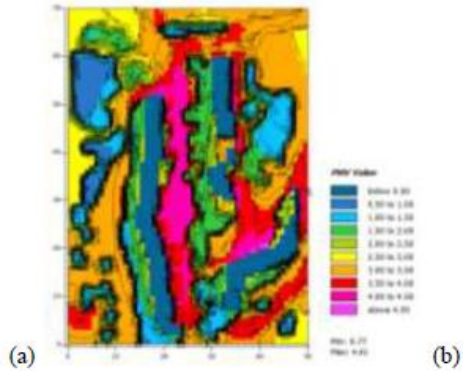

Fig. 5. Comparison between (a) state of art (before) and (b): PMV value d building shift, from 4.00 (magenta) to 2.5-3.0 (yellow-orange) sh

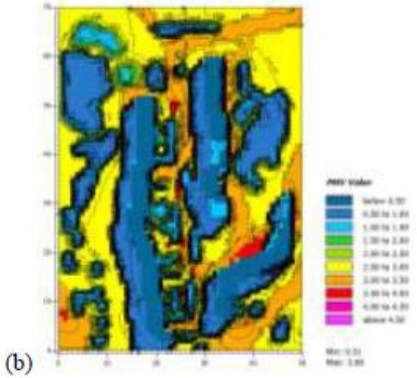

alue distribution. How it can be observed PMV values on street between e) showing the effectiveness of pavement albedo improvement.

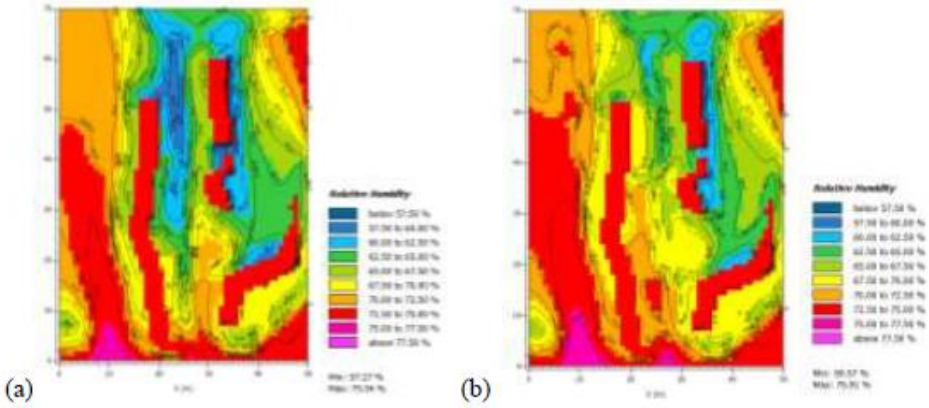

Fig. 3. Comparison between (a) state of art (before) and (b): Relative Humidity distribution

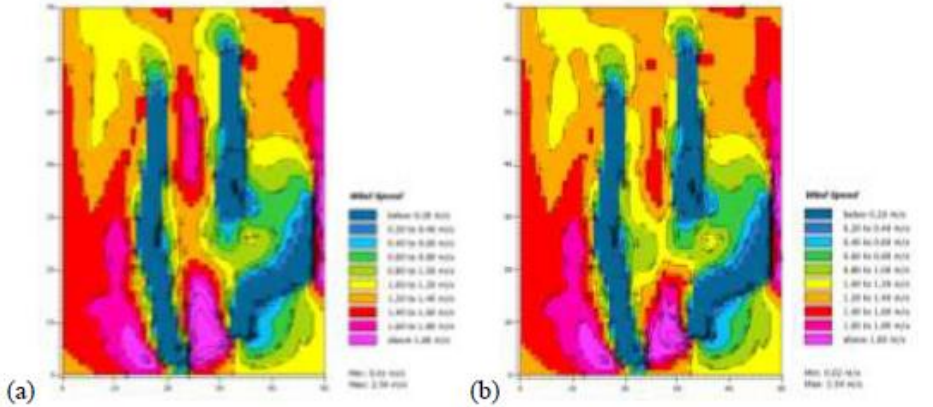

Fig. 4. Comparison between (a) state of art (before) and (b): Wind Speed distribution

OMM Outdoor Microclimate Map

Fig. 2. The site layout before (a) and after (b) intervention (c, d) (credits: L. Ferrari, D. Galassi)

ailable online at www.sciencedirect.com

ScienceDirect

Energy Procedia 111 (2017) 500 – 509

Energy Procedia

ce on Sustainability in Energy and Buildings, SEB-16, 11-13 September 2016, Turin, ITALY

A study on the use of outdoor microclimate map to address design solutions for urban regeneration

Jacopo Gaspari[a,*], Kristian Fabbri[a]†

[a]Department of Architecture, University of Bologna, viale Risorgimento 2, Bologna 40136, Italy

OMM Outdoor Microclimate Map

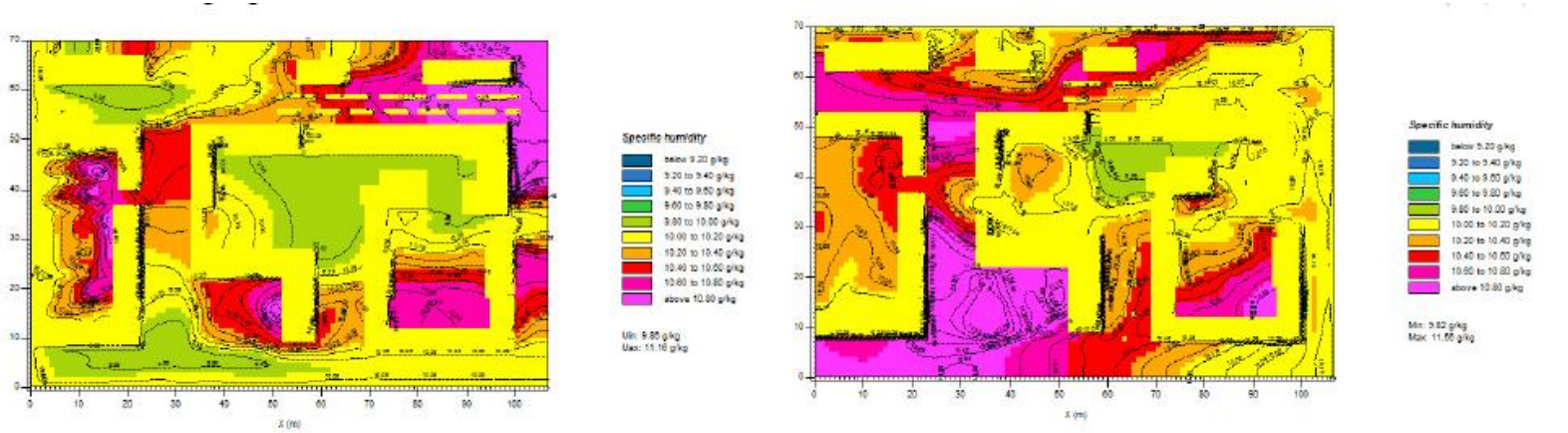

Fig. 6. Specific Humidity in g/kg (a) before; (b) after.

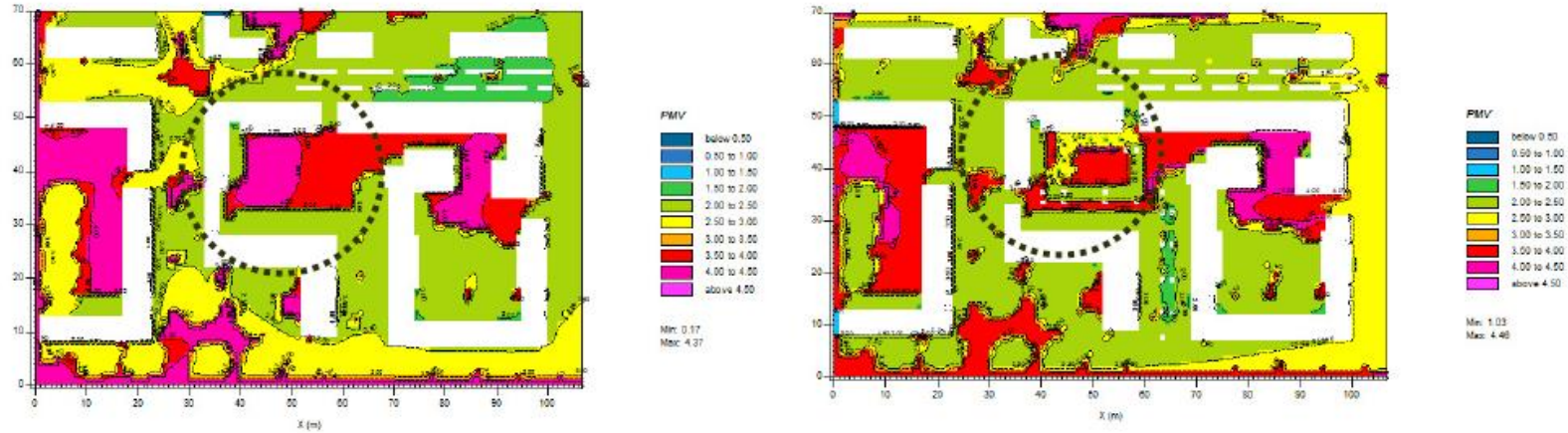

Fig. 7. Predicted Mean Vote (PMV) index (a) before; (b) after.

Il caso Piazza Bufalini a Cesena (referendum)

Outdoor Microclimate Map to compare an open space design: the case study of Piazza Bufalini in Cesena.

Authors

Kristian Fabbri Department of Architecture, University of Bologna (Italy) e-mail: kristian.fabbri@unibo.it
Martina Lucchi Landscape architect, Paesaggista, Cesena (Italy) e-mail: martinalucchi03@gmail.com

- **Stato di fatto**
- **Progetto con mantenimento lecci**
- **Progetto con nuovi alberi e abbattimento lecci**

Il caso Piazza Bufalini a Cesena (referendum)

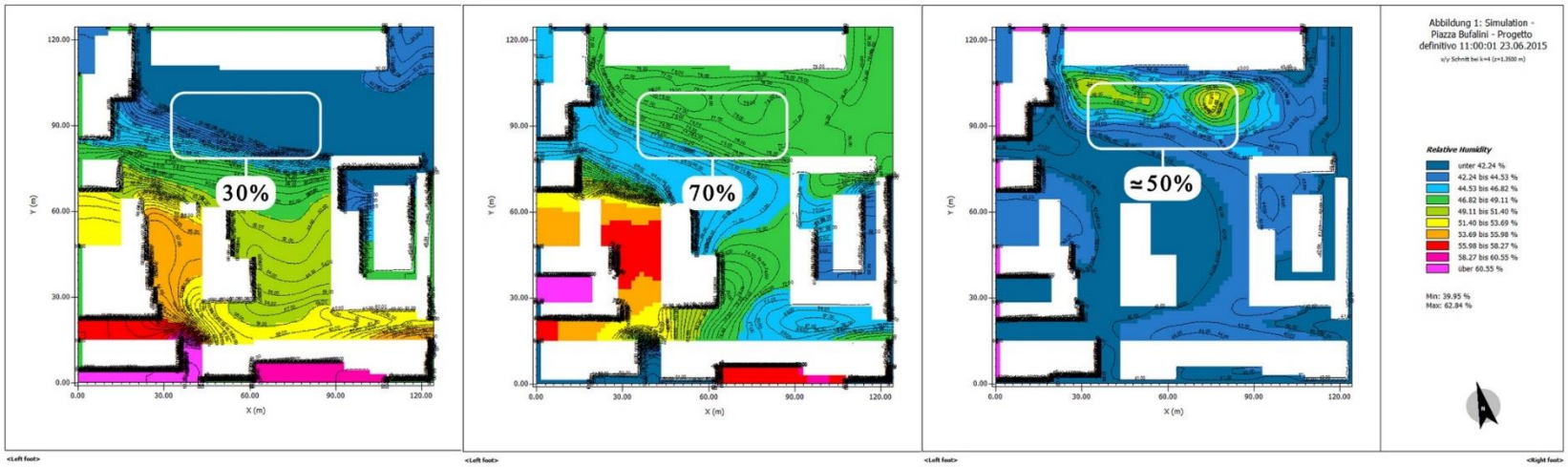

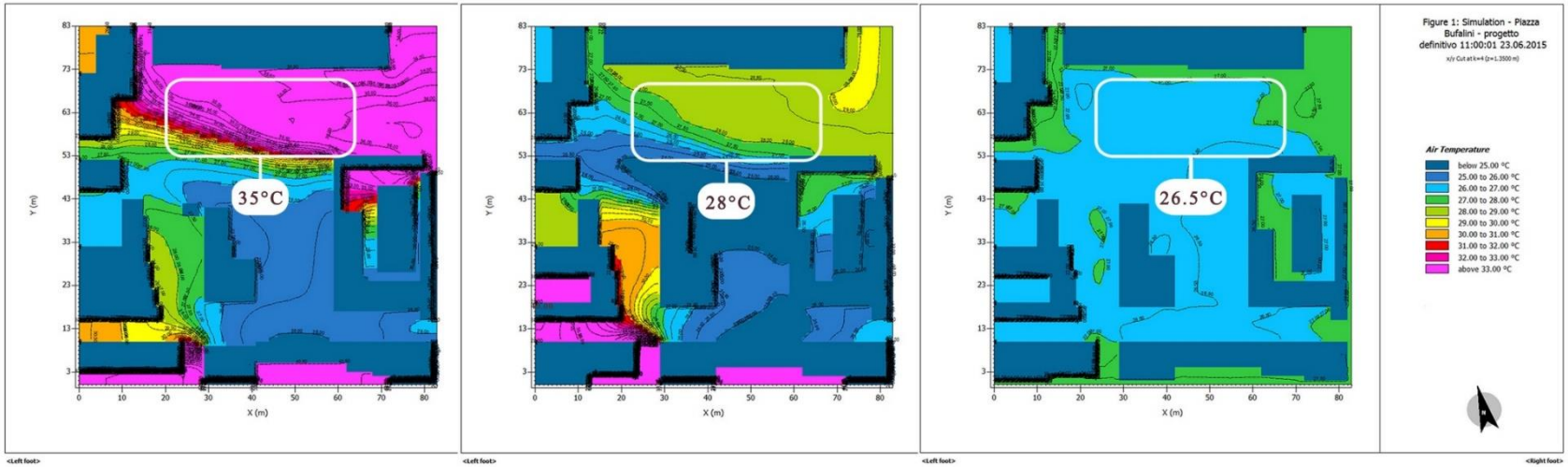

Il caso Piazza Bufalini a Cesena (referendum)

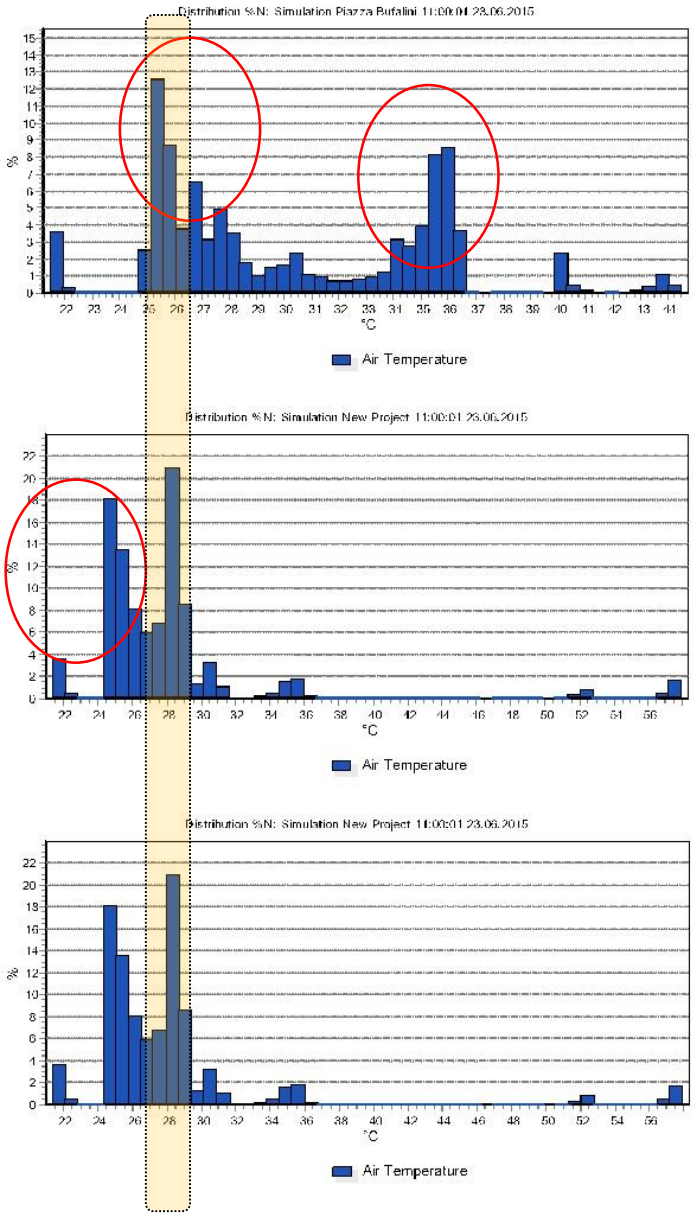

- **Stato di fatto**
- **Progetto con mantenimento lecci**
- **Progetto con nuovi alberi e abbattimento lecci**

Scenario (A)

Scenario (B)

Scenario (C)

Grazie

Arch. Kristian Fabbri www.kristianfabbri.com info@kristianfabbri.com